

Morpho-functional study of the hypothalamic proline-rich polypeptide apoptotic activity against mouse Ehrlich ascites carcinoma

S. ABRAHAMYAN¹, I. SAHAKYAN¹, N. TUMASYAN¹, N. KOCHARYAN¹, A. SIMONYAN²,
R. AROUTIOUNIAN², G. CHAILYAN³, S. CHAILYAN¹, T. DAVTYAN⁴ and K. GALOIAN⁵

¹Laboratory of Histochemistry and Functional Morphology, Institute of Biochemistry after H. Buniatian, NAS RA, 0014 Yerevan; ²Department of Genetics and Cytology, Faculty of Biology, Yerevan State University, 0025 Yerevan, Republic of Armenia; ³Department of Immunology, Institute for Molecular Medicine, Huntington Beach, CA 92647, USA; ⁴Analytical Laboratory Branch, Scientific Centre of Drug and Medical Technology Expertise after Academician E. Gabrielyan CJSC, 0051 Yerevan, Republic of Armenia; ⁵Department of Orthopedic Surgery, University of Miami, Miller School of Medicine, Miami, FL 33136, USA

Received April 12, 2019; Accepted March 20, 2020

DOI: 10.3892/or.2020.7604

Abstract. A new type of bioactive polypeptides of the neurosecretory hypothalamus called proline-rich peptides (PRPs), which are isolated from bovine neurosecretory granules of the neurohypophysis, are synthesized in the form of a common precursor protein (neurophysin vasopressin-associated glycoprotein). Proline-rich polypeptide 1 (PRP-1; also known as galarmin) is comprised of 15 amino acids residues, and has been suggested to possess anti-neurodegenerative, immunoregulatory, hematopoietic, antimicrobial and antitumor properties. The cytostatic, antiproliferative effect of PRP-1 was demonstrated in the human chondrosarcoma JJ012 and triple negative breast carcinoma MDA MB 231 cell lines. PRP-1 action is disease and tissue specific. To further explore the antitumorigenic and possible cytotoxic effects of PRP-1, a morpho-functional study on the effect of PRP-1 on a mouse Ehrlich ascites carcinoma (EAC) model was conducted. The PRP-1-induced morphological features of EAC cells confirmed the apoptotic nature of PRP-1, as manifested by cell shrinkage, membrane blebbing, chromosome condensation (pyknosis) and nuclear fragmentation (karyorrhexis). The effect of PRP-1 on the number of tumor cells incubated for 24 h and their viability

in trypan blue-stained samples lead to a 44% reduction in the number of viable cells on day 11 post-inoculation vs. 22% inhibition of viable cells after PRP-1 treatment (0.1 $\mu\text{g/ml}$) on day 7 post-inoculation. Apoptosis experiments using an Annexin V-cyanine 3 apoptosis detection kit indicated that 24 h incubation with 0.1 $\mu\text{g/ml}$ PRP-1 caused a significant increase in the number of apoptotic cells, reaching 50.33%, compared to 8.33% in the sample control on day 7 post-inoculation.

Introduction

A new type of bioactive polypeptides of the neurosecretory hypothalamus, the proline-rich polypeptides (PRPs), were isolated in 2001 from bovine neurohypophysis neurosecretory granules (1,2). PRPs are synthesized from a common precursor, namely neurophysin vasopressin-associated glycoprotein. The mTORC1 inhibitor proline-rich polypeptide 1 (PRP-1; also known as galarmin) is a short 15-amino acid neuropeptide (sequence, Ala-Gly-Ala-Pro-Glu-Pro-Ala-Glu-Pro-Ala-Gln-Pro-Gly-Val-Tyr) with neuroprotective, immunomodulatory (3,4), antiviral, anti-inflammatory (5), antibacterial (6), hematopoietic (7) and antitumor properties (8-10,11-14).

PRP-1 was identified as a ligand for innate immunity pattern recognition Toll-like receptors 1,2 and 6, and the mucosal protein mucin 5B (15). PRP-1 caused significant upregulation of tumor suppressor genes and miRNA with tumor suppressor function and downregulation of onco-miRNAs in the human chondrosarcoma JJ012 cell line (11,13). The antiproliferative effect of PRP-1 was caspase-3-independent and cytostatic by nature in the bulk human chondrosarcoma cell population (16) and in triple negative breast cancer (10). The antitumor function of PRP-1 was demonstrated to be organ-specific, since it did not display any effect on glioblastoma (12).

The Ehrlich ascites carcinoma (EAC) is a common undifferentiated tumor with rapid growth rate and sensitivity to chemotherapy (17). Ehrlich tumors originate from spontaneous murine mammary adenocarcinomas and adapt to ascites form

Correspondence to: Dr K. Galoian, Department of Orthopedic Surgery, University of Miami, Miller School of Medicine, 1600 NW 10th Avenue, S 8012, Miami, FL 33136, USA
E-mail: kgaloian@med.miami.edu

Dr S. Abrahamyan, Laboratory of Histochemistry and Functional Morphology, Institute of Biochemistry after H. Buniatian, NAS RA, P. Sevak 5/1, 0014 Yerevan, Republic of Armenia
E-mail: silva.abrahamyan@gmail.com

Key words: PRP-1, galarmin, Ehrlich ascites carcinoma, mice, histology, fluorescence, apoptosis, Annexin V-Cy3

by intraperitoneal (ip) serial passages. The EAC model is widely used in experimental cancer due to its high efficiency in producing free neoplastic cells and its accuracy in terms of survival time (18). The aim of the present study was *in vitro* exploration of the effect of PRP-1 on EAC cells collected from the ascitic fluid of EAC cell-bearing mice.

Materials and methods

EAC mouse model. The ascitic fluid of [2 to 3-month-old male white Swiss (SWR/J) mice weighing 20 ± 2 g] with the EAC model was provided by the Laboratory of Toxicology and Experimental Chemotherapy (Institute of Fine Organic Chemistry, National Academy of Sciences of Armenia). Mice were inoculated with EAC-E2G8 tumor cells (obtained by the Hebei Medical University scholars from the Beijing Cancer Institute EAC) to produce the EAC model.

The ascitic fluid containing the EAC cells was obtained from the peritoneal cavity of mice on days 7 (n=10) and 11 (n=10) after tumor growth, and then used for *in vitro* experiments at the laboratory of Histochemistry and Functional Morphology (Institute of Biochemistry after H. Buniatian, NAS RA).

Culture of cell suspension. The EAC cell suspensions obtained from the peritoneal cavity of mice (which closely mimic *in vivo* conditions) and suspensions containing EAC cells isolated by centrifugation were used. Ascitic fluid was centrifuged at $300 \times g$ for 5 min at 18–20°C.

Then, the supernatant was discarded, and the cells were washed in Hanks' Balanced Salt Solution buffered with phosphate (pH 7.4) (cat. no. 55037C; Sigma-Aldrich; Merck KGaA). Subsequently, the cells were re-suspended in Hanks' Balanced Salt Solution to a concentration of 5×10^6 cells/ml in RPMI-1640 medium and grown in tissue culture dishes until ~80% confluence in RPMI-1640 culture medium (BioloT, Ltd.) containing 10% heat-inactivated fetal bovine serum, 50 U/l penicillin and 1% L-glutamine. The cell suspensions were incubated at 37°C and 5% CO₂ with constant shaking. Control samples (n=3) untreated with PRP-1 and experimental samples with single administration of 0.1 µg/ml PRP-1 (n=3) and 1 µg/ml PRP-1 (n=3) were cultured for 24 and 72 h in unchanged culture medium. Daily quantification of the total and viable number of EAC cells was carried out. Each condition was tested in triplicate.

Tumor cell count. For the culture of EAC cells, 5×10^6 cells were obtained from the suspension containing numerous tumor cells, by diluting it in RPMI-1640 medium. The cells were counted in a Neubauer chamber (19).

Histological and immunohistological staining. A light digital microscope (M10; Motic) was used for histological and immunohistochemical investigations.

Histological staining

Trypan blue (Tr-BI) staining. The number of viable cells in the suspension was determined by the method of exclusion with trypan blue (diazo live dye, at a concentration 0.4%) (20). Using the Tr-BI staining method, the percentage of dead and alive cells was calculated after 24 h of incubation in the control

samples and those treated with PRP-1 at 0.1 and 1 µg/ml concentrations.

Haematoxylin and eosin (H&E) staining. EAC suspension smears were fixed in 96% ethanol for 10 min at room temperature; dehydrated by passing through decreasing concentrations of alcohol baths (96 and 75%) and distilled water, stained in haematoxylin for 5 min at room temperature, washed in tap water for ≤5 min, stained in 1% eosin for 1 min at room temperature, washed in tap water for 2 min, dehydrated in increasing concentrations of ethanol (75 and 96%), cleared in xylene two times, and mounted with DPX (cat. no. 06522; Sigma-Aldrich; Merck KGaA) (21).

Giemsa staining. For staining the smears of the EAC cell suspension, Giemsa stain was used at a 1:20 ratio. To produce a 1:50 dilution of Giemsa stain, 1 ml stock solution of Giemsa stain was added to 49 ml phosphate-buffered (pH6.4) solution. The smears were dried in air and covered in DPX (22).

Papanicolaou staining. A drop of the EAC cell suspension was spread on a glass slide, dried in air and fixed in 95% ethyl alcohol for 30 min at room temperature. Slides were then incubated in 70 and 50% ethanol followed by distilled water, stained in Harris hematoxylin for 4 min at room temperature, rinsed briefly in warm (20–30°C) distilled water for 4 min, placed in tap water for 6 min, rinsed in distilled water, and incubated in 50, 70, 80 and 95% ethanol. Then, the slides were stained in EA-50 for 2 min at room temperature; rinsed three times with 95% ethanol, dehydrated in absolute alcohol, followed by equal parts of absolute alcohol and xylol, cleared in xylol, and mounted with DPX (23).

Fluorescence microscopy. Determination of the tumor cell apoptosis rate was performed using the Annexin V-Cy3 apoptosis Detection Kit (product no. APOAC; Sigma-Aldrich KGaA). The non-fluorescent compound 6-carboxyfluorescein diacetate (6-CFDA) enters viable cells, is hydrolyzed by esterases to the fluorescent compound 6-carboxyfluorescein (6-CF) and then retained in the cytoplasm. Dead cells do not exhibit uptake of 6-CFDA and have an increased efflux of the free 6-CFDA. The apoptosis assay is based upon double staining with cyanine 3 (Cy3)-conjugated Annexin V and the vital dye 6-CFDA. The assay discriminates viable cells (Cy3⁺/6-CF⁺) from apoptotic (Cy3⁺/6-CF⁻) and dead (necrotic) cells (Cy3⁻/6-CF⁻). There are three possible outcomes: i) living cells that only stain with 6-CF (green); ii) necrotic cells that only stain with AnnexinV-Cy3 (red); and iii) cells starting the apoptotic process, which stain both with Annexin V-Cy3 (red) and 6-CF (green), resulting in yellow-orange stain (24). A total of 400 cells/sample were analyzed. Data represent 3 independent experiments (25).

The nuclear counterstain method with DAPI fluorescent staining dye (cat. no. D1306; Thermo Fisher Scientific, Inc.) was used to confirm the PRP-1 nuclear localization in the cultured EAC cells and detection was performed using the ABC immunohistochemical method.

Immunohistochemical staining. The avidin-biotin complex (ABC) immunohistochemical method was applied for

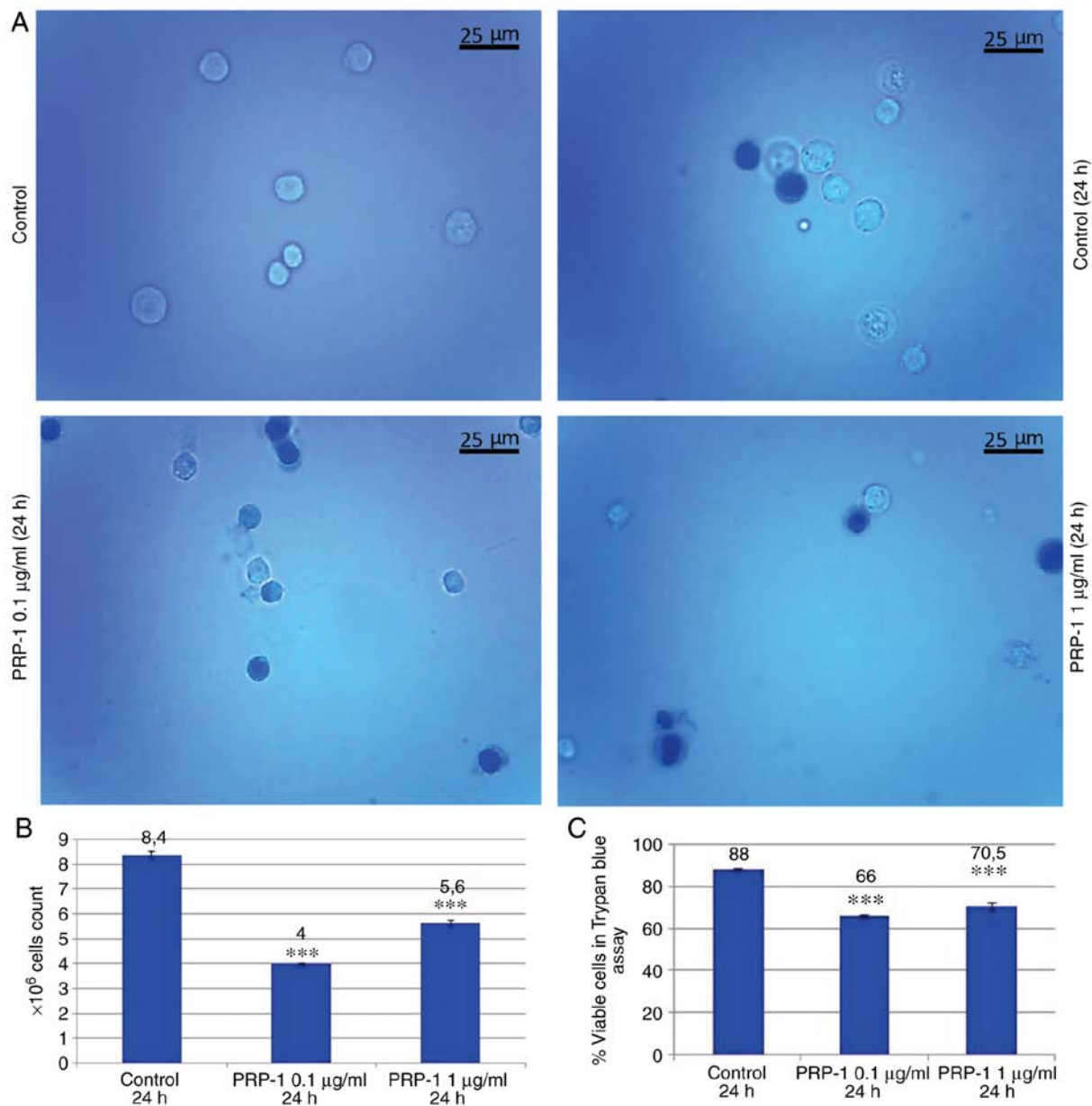


Figure 1. Effect of the hypothalamic PRP-1 on the growth and viability of mouse isolated EAC cells on the 7th day of tumor growth: Histological method with Tr-BI staining. (A) Viable EAC cells were revealed in the control samples before their culture (control). Various dead Tr-BI-positive tumor cells were detected among the viable cells in the non-treated control samples 24 h after culture (control 24 h). An increased number of Tr-BI-positive dead cells was evident 24 h after 0.1 and 1 μg/ml PRP-1 administration. The PRP-1 inhibitory effect (0.1 and 1 μg/ml) on the number of (B) total and (C) viable tumor cells treated for 24 h was statistically significant according to the Tr-BI exclusion test in comparison with the findings in the untreated control cells. Data are presented as the mean ± standard deviation (n=3), and represent ≥3 independent experiments. ***P<0.001, significant difference compared to the control at 24 h. Tr-BI, trypan blue; PRP, proline-rich peptide; EAC, Ehrlich ascites carcinoma.

detection of PRP-1 localization in cancer cells using antiserum produced at our laboratory (Institute of Biochemistry NAS, Armenia) against synthetic PRP-1 (26). After rinsing several times in PBS, the samples were treated with Triton X-100 for 45 min to permeabilize, 0.3% hydrogen peroxide for 30 min to suppress the background peroxidase activity, and normal goat serum (1:30; cat no. S-1000; Vector Laboratories, Inc.) for 45 min to block non-specific binding of antibodies. Then, the samples were incubated in primary antiserum [anti-PRP-1; 1:2,000; produced at the laboratory of Histochemistry and Functional Morphology (Institute of Biochemistry, NAS, Armenia)] for 24 h at 4°C, secondary antiserum (biotinylated goat anti-rabbit immunoglobulin; 1:200; cat. no. BP-9100) for

45 min; and streptavidin (1:100; cat. no. SA-5000; both from Vector Laboratories, Inc.) for 45 min at room temperature. Immunoreactivity (IR) was revealed by 0.02% 3,3'-diaminobenzidine tetrahydrochloride (DAB) (product no. D5905; Sigma-Aldrich; Merck KGaA) and 0.6% nickel ammonium sulfate diluted in 50 mM Tris-HCl buffer (pH 7.6) in the presence of 0.03% hydrogen peroxide as an oxidant. Both primary and secondary antisera were diluted in PBS containing 0.1% bovine serum albumin (BSA) (product no. 05470; Sigma-Aldrich; Merck KGaA) and 0.01% sodium azide. All incubations, except for the incubation with normal goat serum, were separated by washes in PBS. The slides were mounted in DPX medium and the results were analyzed using light

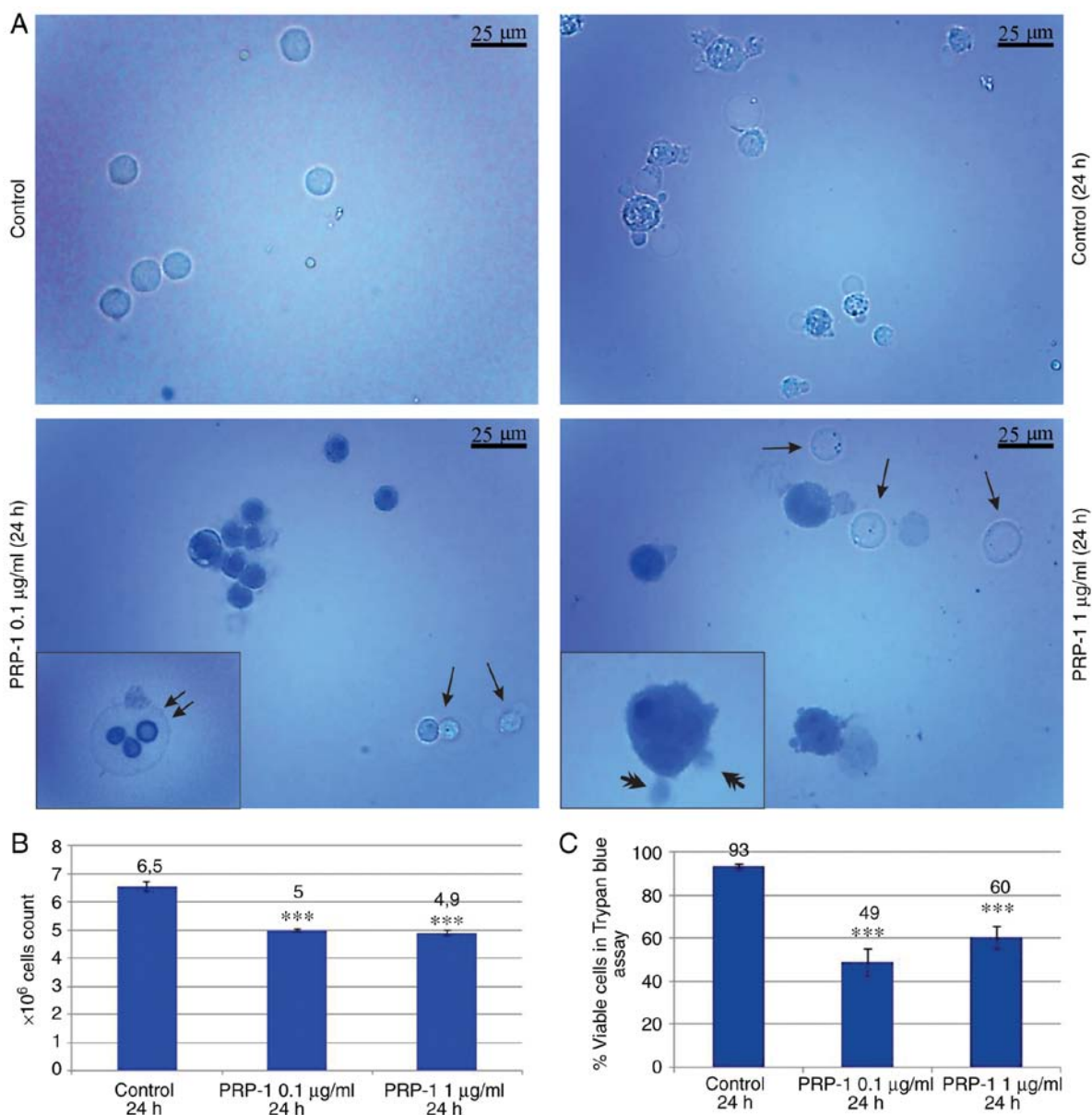


Figure 2. Effect of the hypothalamic PRP-1 on the growth and viability of mouse isolated EAC cells on the 11th day of tumor growth: Histological method with Tr-BI staining. (A) Viable EAC cells were detected before their culture (control). EAC control cells after 24 h of incubation were mainly viable, although various dead Tr-BI-positive cells were present (control 24 h). In samples treated with 0.1 and 1 µg/ml PRP-1, an increased number of Tr-BI-positive non-viable cells was detected, along with various viable cells (arrows), apoptotic cells with fragmented nuclei (double arrows) and various Tr-BI-positive cells surrounded by apoptotic bodies (arrow heads). The PRP-1 inhibitory effect (0.1 and 1 µg/ml) on the number of (B) total and (C) viable tumor cells treated for 24 h was statistically significant according to the Tr-BI exclusion test in comparison with the findings in the untreated control cells. Data are presented as the mean ± standard deviation (n=3), and represent ≥3 independent experiments. ***P<0.001, significant difference compared to the control at 24 h. Tr-BI, trypan blue; PRP-1, proline-rich polypeptide 1; EAC, Ehrlich ascites carcinoma.

microscopy at x100, x400 and x1,000 magnifications. To confirm immunospecificity for PRP-1, the primary antiserum was replaced by normal goat, phosphate buffer or PRP-1 antiserum pre-absorbed with synthetic PRP-1, synthesized at our laboratory (Institute of Biochemistry, NAS, Armenia) for the negative control experiments.

PRP-1 antiserum production and affinity chromatography purification

Antiserum production. For immunization 1 to 1.5-year old wild male ~3-4 rabbits [*Oryctolagus cuniculus* (Linnaeus, 1758)] of the Californian breed, weighing 2 kg were used. Animal immunization was performed using pentobarbital

(Nembutal; serial no. 71308321 and registration no. 0285003) anesthesia at a dose of 30-35 mg/kg. The Institutional Animal Ethics Committee of Buniatian Institute of Biochemistry of the NAS (IRB 0001621; IORG0009782) provided approval for the use of the animals. The rabbits woke up normally and behaved naturally after the procedures which lasted 10-15 min, were performed. The rabbits were housed in cages (cage model RBB-S-01) comprised of 2 sections of size, 600x450x450 mm, separated by a removable partition, one animal in each section. Rabbits were maintained at a room temperature of 18-22°C and a relative humidity of 55-65%. Rabbits were fed twice a day, morning and evening with a daily diet which consisted of: Unlimited access to hay or grass, a

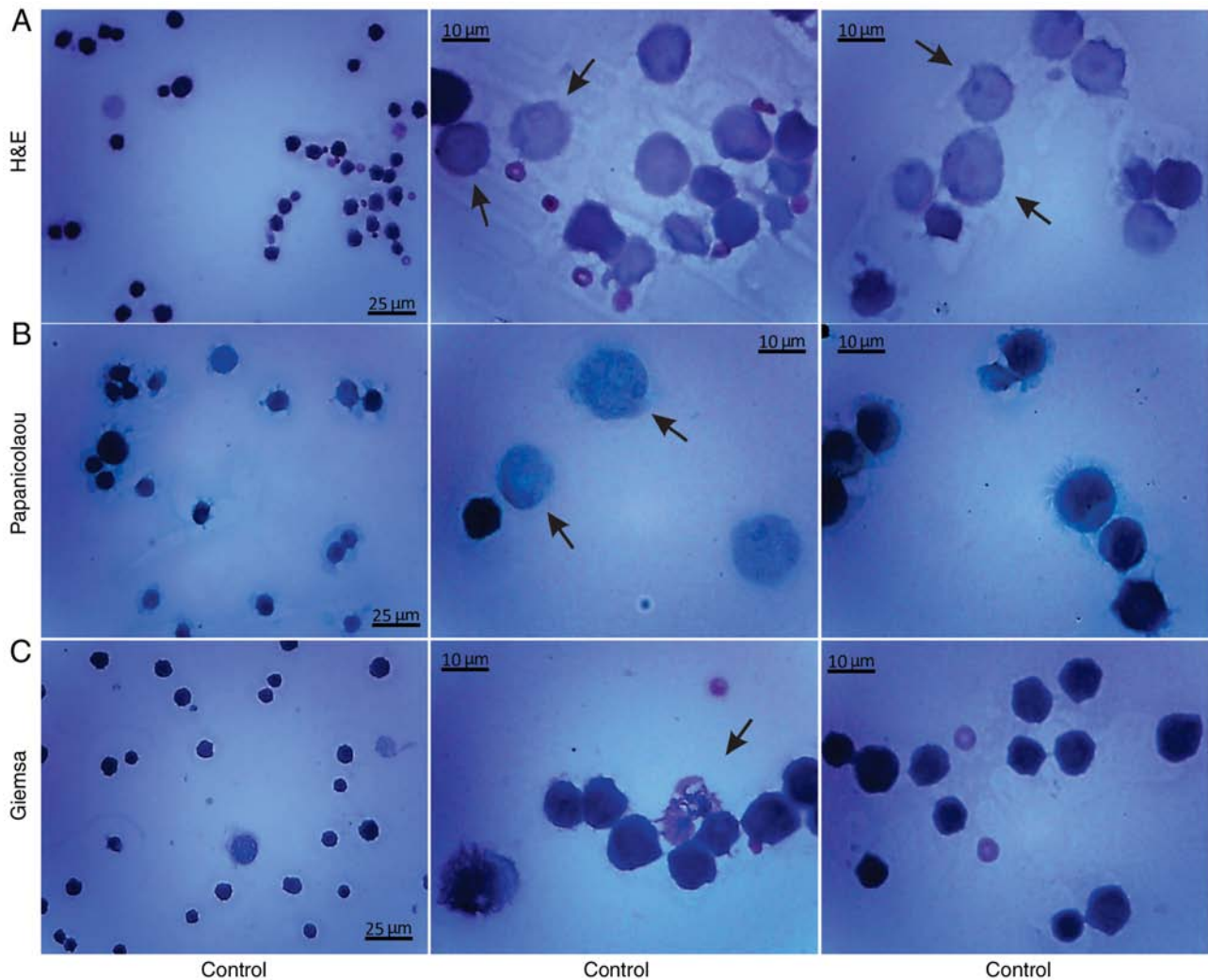


Figure 3. Histological study of mouse EAC cells in suspension obtained directly from the peritoneal cavity of mice on the 7th day of tumor growth before culture: Histological methods with (A) H&E, (B) Papanicolaou and (C) Giemsa staining. Stained in red, small erythrocytes not containing nuclei and weakly-stained macrophages (arrows) were observed next to strongly-stained EAC cells. EAC, Ehrlich ascites carcinoma; H&E, hematoxylin and eosin.

handful of fruits, vegetables or leafy plants and a small amount of high-quality commercial mix (for rabbits) or granules (up to 25 g per kg of rabbit body weight). The rabbits were used once more to obtain a new portion of PRP-1-antiserum with higher titration.

Antiserum against synthetic PRP-1 was obtained according to the method by Ambrosius (27). The PRP-1-BSA conjugate, was mixed with 1 mg/0.2 ml Freund's Complete Adjuvant (product no. F5881; Sigma-Aldrich; Merck KGaA), until a homogenous emulsion was achieved (28), and then injected in equal portions into the lower extremities of rabbits in the region of both popliteal lymph nodes. Immunization was repeated 1 month later by injecting a freshly prepared emulsion (1 mg PRP-1-BSA in 1 ml phosphate buffer, pH 7.4) in the following locations: Into the region of the left popliteal lymph node (0.4 ml), into the auricular vein (0.2 ml) and, intramuscularly on the right side (0.4 ml). After reimmunization, blood samples were obtained from the auricular vein on days 7, 9 and 11 from the rabbits, mixed and kept in the refrigerator (at +4°C). Then 10 ml of this mixture was lyophilized. The specificity of the antiserum was tested by immunodiffusion and ELISA (29).

PRP-1 antiserum affinity chromatography purification. PRP-1 antiserum affinity chromatography purification was performed using AminoLink™ Plus Immobilization kit (Thermo Fisher Scientific, Inc.) according to the manufacturer's instructions.

Statistical analysis. Statistical analysis was performed using the statistical package Statgraphics Centurion 16.2 (StatPoint Technologies, Inc.). The results were compared with those of the control, and the Student's t-test was used to estimate the statistical significance of the data. Data were presented as the mean \pm standard deviation. $P < 0.05$ was considered to indicate a statistically significant difference.

Results

Histological (Tr-BI, H&E, Giemsa, Papanicolaou and Annexin V-Cy3 apoptosis detection stains) and immunohistochemical (ABC) methods were used in the present study to investigate the antitumorigenic effect of PRP-1 in EAC cells. EAC suspensions, including those obtained from the peritoneal cavity of mice (since it closely resembles *in vivo* conditions) and those containing isolated EAC cells, were

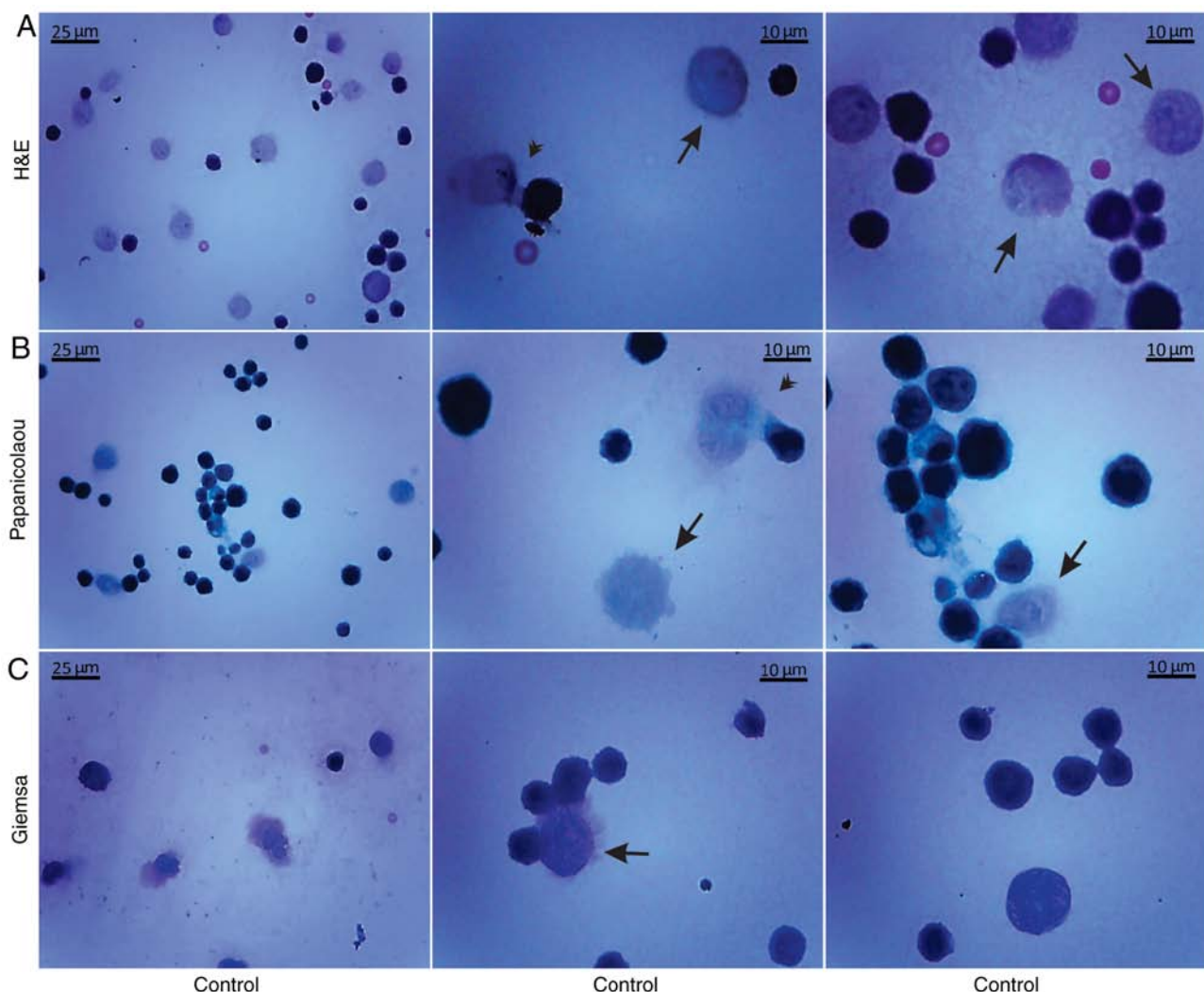


Figure 4. Histological study of mouse EAC cells in suspension obtained from the peritoneal cavity of mice on the 11th day of tumor growth before culture: Histological methods with (A) H&E, (B) Papanicolaou and (C) Giemsa staining. Weakly-stained cells, possibly macrophages (arrows), were mainly located in close contact with strongly-stained EAC cells. Various cells exhibiting phagocytosis were also observed (arrowheads). EAC, Ehrlich ascites carcinoma; H&E, hematoxylin and eosin.

used. The effect of 0.1 and 1 $\mu\text{g/ml}$ PRP-1 was studied on the isolated EAC cells of mice on days 7 and 11 of tumor growth and cultured for 24 and 72 h.

Histological study. Light microscopy and histological staining with Tr-BI experiments were used to reveal the percentage of dead and alive cells after 24 h of incubation in the control samples and those treated with PRP-1 at the aforementioned concentrations.

Statistical analysis of the tumor growth at 24 h confirmed the PRP-1 antitumorigenic effect on EAC cells. Figs. 1 and 2 revealed a decrease in the number of total EAC cells when treated with PRP-1 (0.1 and 1 $\mu\text{g/ml}$), indicating the anti-proliferative activity of PRP-1 in comparison with the findings in the 24 h untreated control samples. Concurrently, the number of viable EAC cells treated with PRP-1 was decreased compared with that in the control group. On day 7 post-inoculation, the number of total cells was 5×10^6 , and increased to 8×10^6 , with viable cells comprising 88% of the cell population, whereas in the 0.1 $\mu\text{g/ml}$ PRP-1-treated samples, the total number of cells was reduced to 4×10^6 , where viable cells accounted for 66% of

the total population. Thus, PRP-1 inhibited the growth of viable cells by 22% (Fig. 1B and C). On day 11 post-inoculation, the total number of cells increased from 5×10^6 to 6.5×10^6 , of which 93% were viable in the 24 h control, while in the PRP-1-treated samples, that number was 5×10^6 , with only 49% of viable cells, thus indicating an inhibition of viable cells by 44% caused by PRP-1 (Fig. 2B and C). The difference between the effect of 0.1 and 1 $\mu\text{g/ml}$ PRP-1 was clearly visible when comparing the total number of EAC cells on the 7th day of inoculation indicating the more effective anti-proliferative action of 0.1 $\mu\text{g/ml}$ PRP-1. Thus, since similar results were obtained with the 11th day inoculation, 0.1 $\mu\text{g/ml}$ PRP-1 was selected for further use.

Histological methods with H&E, Papanicolaou and Giemsa staining were applied to examine the morphological characteristics of the non-cultured control EAC cells obtained from the peritoneal cavity of mice on days 7 and 11 of tumor growth (Figs. 3 and 4). Small erythrocytes not containing nuclei, and macrophages were observed next to EAC cells. Macrophages exhibiting phagocytosis were also observed, located mainly in close contact with EAC cells.

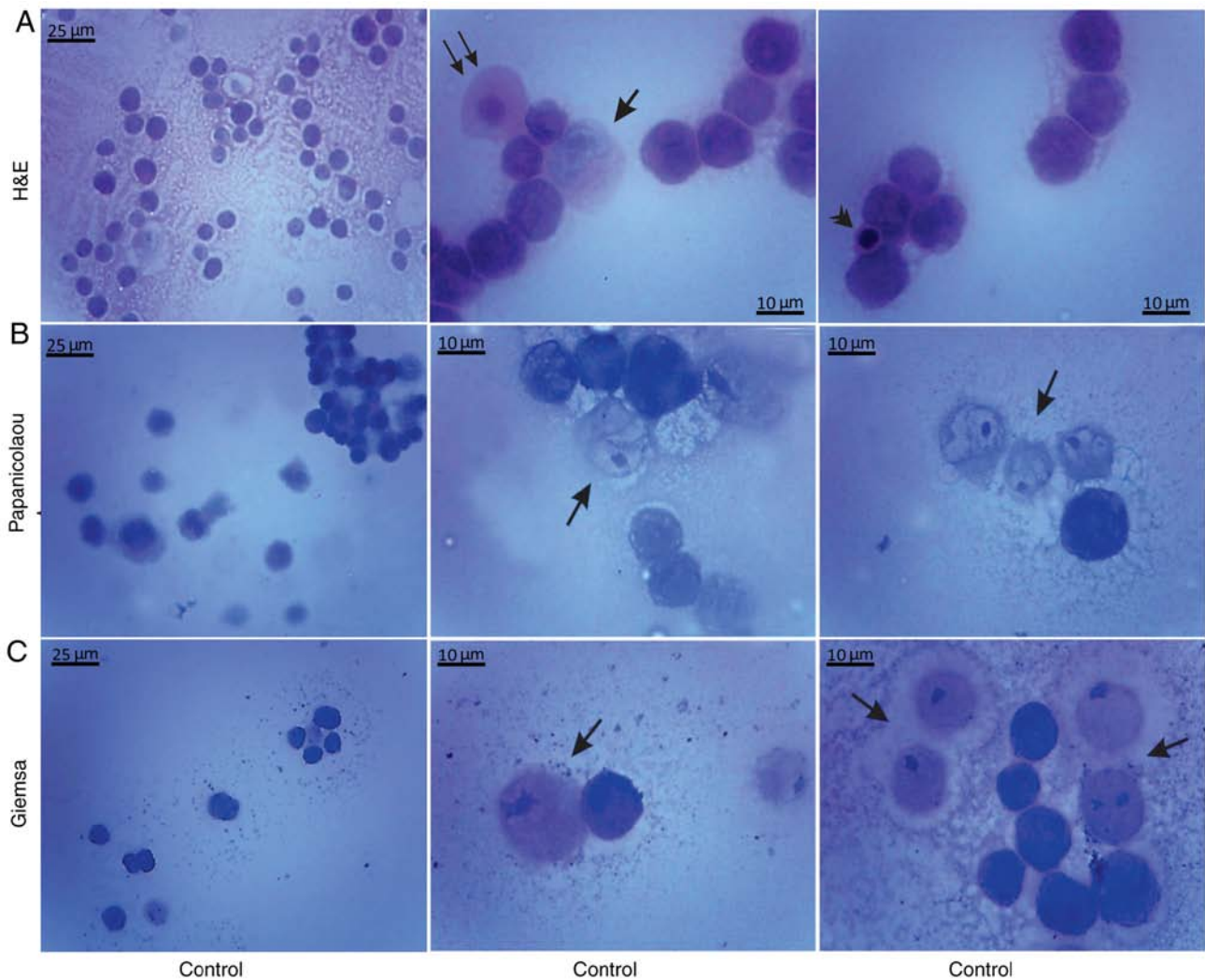


Figure 5. Morphological characteristics of isolated mice not treated with PRP-1 EAC cells on the 7th day of tumor growth before culture: Histological methods with (A) H&E, (B) Papanicolaou and (C) Giemsa staining. (A) Control EAC cells exhibiting a typical tumor morphology, i.e. linked with each other by cytoplasmic bridges and centrally-located large nuclei in different stages of mitosis. In addition, macrophages (arrows), normoblasts (double arrows) and an apoptotic body (arrowhead) containing basophilic nuclei were observed. Cells, perhaps macrophages (arrows), weakly-stained both with (B) Papanicolaou and (C) Giemsa were located in close proximity to strongly-stained EAC cells. PRP-1, proline-rich polypeptide 1; EAC, Ehrlich ascites carcinoma; H&E, hematoxylin and eosin.

Morphological evaluation of the isolated, by centrifugation, non-cultured control EAC cells was performed by the aforementioned histological methods on days 7 (Fig. 5) and 11 (Fig. 6) of tumor growth. The isolated control EAC cells exhibited a typical tumor morphology, i.e. linked with each other by cytoplasmic bridges, and centrally-located large nuclei in different stages of mitosis were detected. In addition, normoblasts, the apoptotic bodies, as well as macrophages were revealed, located in close proximity to strongly-stained EAC cells. Notably, EAC cells on the 11th day of tumor growth markedly differed from tumor cells on the 7th day after inoculation, since they were larger in size and exhibited pathological mitosis.

To confirm the antitumorigenic effect of PRP-1, histological examination with H&E staining was further conducted, which is widely used in medical diagnosis and cancer detection.

PRP-1-induced morphological features of EAC cells (Figs. 7 and 8) indicated the apoptotic nature of PRP-1 as well, manifested by cell shrinkage, membrane blebbing, nuclear

condensation (pyknosis) and fragmentation (karyorrhexis) as well as by a predominant presence of apoptotic bodies (30-35). There are indications that choice of program of autodestruction occurs before initiation of the irreversible phase of cell response to a lethal signal. The hallmark of apoptosis, externalization of phosphatidylserine, that designates a cell with an 'eat me' message, is the earliest feature of apoptosis triggering (36,37). In necrotic cells this feature is usually registered after plasma membrane destruction; therefore, necrotizing cells are not recognized by phagocytes and they cannot be digested until their intracellular contents are spilled into the extracellular space (38). Thus, statistical analysis of the number of apoptotic and necrotic cells was based on the certain aforementioned morphological features, i.e. the nuclear lysis, activated loss of cell membrane integrity and an uncontrolled release of products of cell death into the extracellular space caused by necrosis (39,40), and the cell shrinkage, membrane blebbing and predominant presence of apoptotic bodies induced by apoptosis (41).

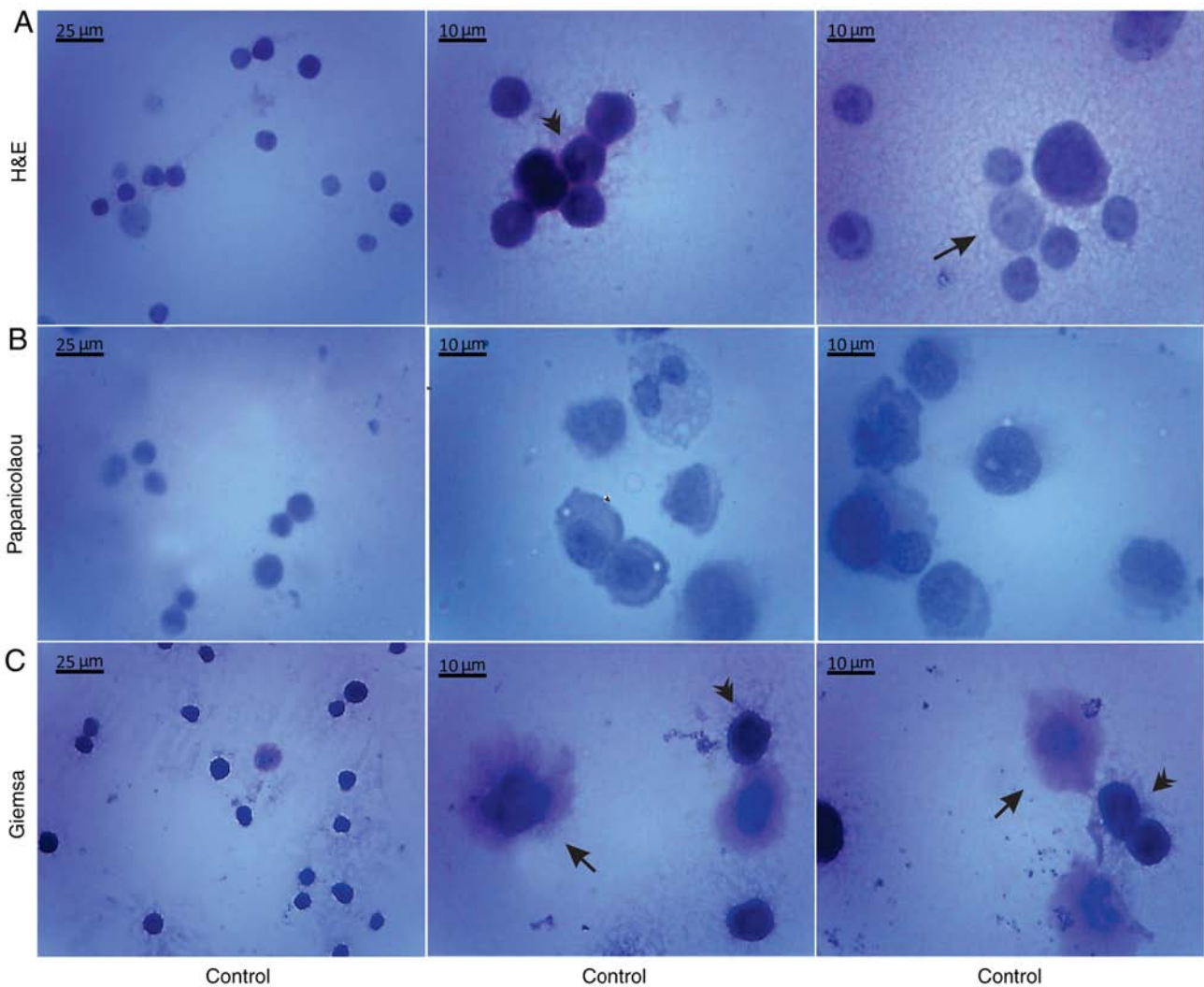


Figure 6. Morphological characteristics of isolated mice not treated with PRP-1 EAC cells on the 11th day of tumor growth before culture: Histological methods with (A) H&E, (B) Papanicolaou and (C) Giemsa staining. (A) EAC control cells linked with each other by reticular bridges exhibited typical features of tumor cells (arrow heads). (B) EAC cells on the 11th day of tumor growth markedly differed from tumor cells on the 7th day after inoculation, since they were larger in size and exhibited pathological mitosis. (C) Tumor cells (arrow heads) and macrophages (arrows) were clearly distinguished by strong staining with Giemsa. PRP-1, proline-rich polypeptide 1; EAC, Ehrlich ascites carcinoma; H&E, hematoxylin and eosin.

In the 7th day inoculated mice EAC cells, PRP-1 induced apoptosis by 70% (0.1 $\mu\text{g/ml}$) and 37% (1 $\mu\text{g/ml}$) at the 24 h culture, in comparison with the control samples (8.7%). At the 72 h culture, PRP-induced apoptosis by 37.3% (0.1 $\mu\text{g/ml}$) and 25.8% (1 $\mu\text{g/ml}$) compared to 1.4% apoptosis in the control samples (Fig. 7). In the control EAC cells of the 11th-day inoculated mice (Fig. 8), cultured for 24 h, apoptosis was 31.2%, whereas in the experimental samples of 0.1 and 1 $\mu\text{g/ml}$ PRP-1, apoptosis was increased to 70.5 and 44.4%, respectively. At the 72 h culture, apoptosis was 6.9% in the control group, against 25.2% for the 0.1 $\mu\text{g/ml}$ PRP-1 group and 9% for the 1 $\mu\text{g/ml}$ PRP-1 group.

On the 7th day post-inoculation a statistically significant increase in the number of necrotic cells was observed after the 24 h 1 $\mu\text{g/ml}$ PRP-1 administration (20.9%) compared to the control (4.5%), whereas no differences were observed between the control and the 0.1- $\mu\text{g/ml}$ PRP-1 (2.7%) samples. The statistically significant decrease of the number of necrotic cells was observed for the 72 h treatment with 0.1 $\mu\text{g/ml}$ PRP-1 (17%) in comparison with both control samples (65.8%) and cells exposed to 1 $\mu\text{g/ml}$ PRP-1 (30.4%).

On the 11th day post-inoculation, a statistically significant increase of the number of necrotic cells was also revealed after the 24 h (23.5%) culture with 1 $\mu\text{g/ml}$ PRP-1 compared to those in the control samples (1%) and experimental samples exposed to 0.1 $\mu\text{g/ml}$ PRP-1 (0.5%). Thus, taking into account the similar data obtained in the control samples, as well as the samples treated with 1 $\mu\text{g/ml}$ PRP-1, further experiments were carried out for the cells with 0.1 $\mu\text{g/ml}$ PRP-1.

Fluorescence microscopy. The apoptosis-related morphological changes were monitored with histological methods (Tr-BI and H&E staining). The data of the statistical analysis observed in EAC cells treated with 0.1 $\mu\text{g/ml}$ PRP-1 was confirmed by fluorescence microscopy with Annexin V-Cy3 staining (Figs. 9A and 10A) in comparison to non-treated control samples at 24 h.

Statistically significant differences between the control and experimental samples in terms of PRP-1-induced apoptosis were observed in EAC cells, as depicted in Figs. 9B and 10B. It was revealed that 24 h of incubation with 0.1 $\mu\text{g/ml}$ PRP-1

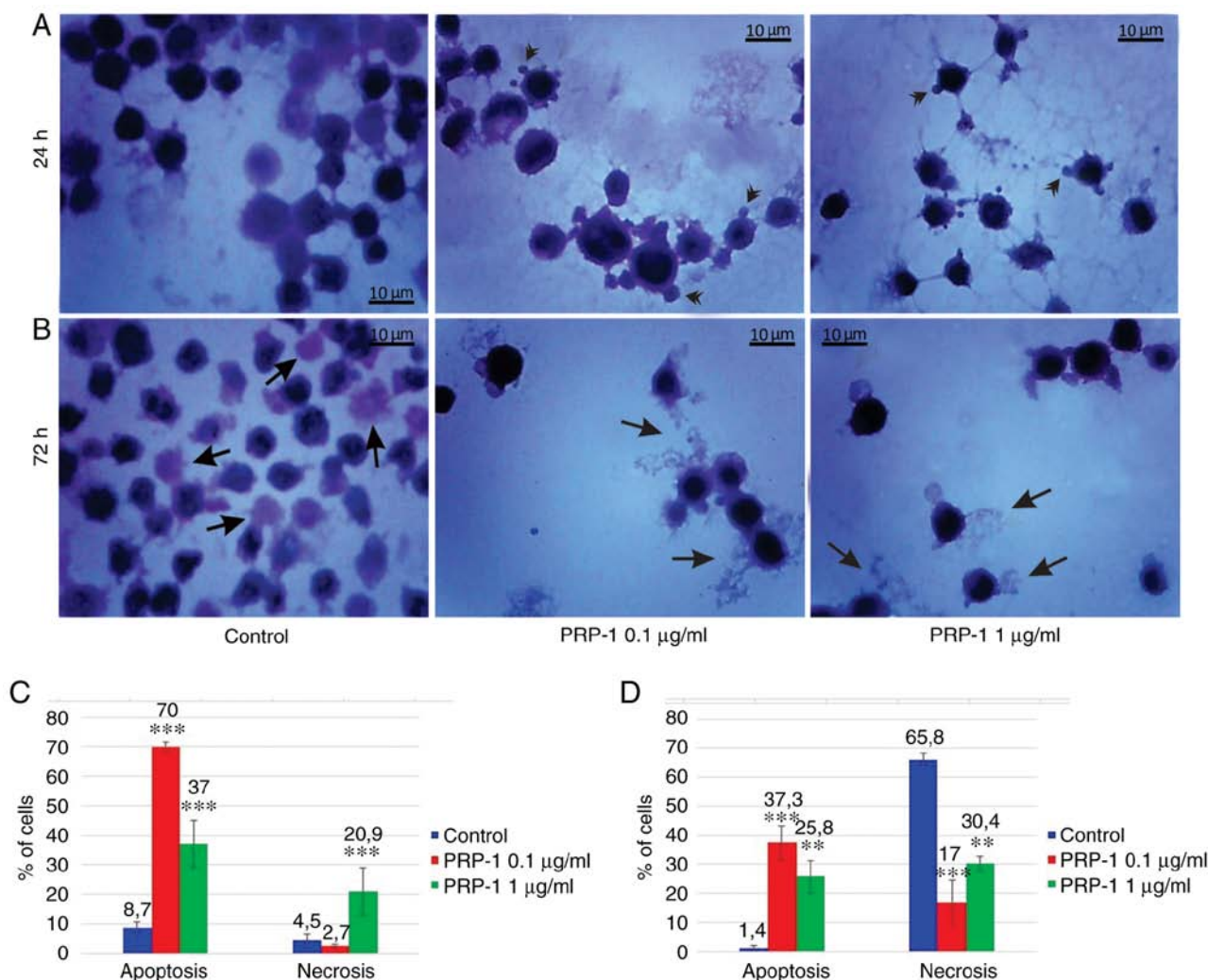


Figure 7. Histological evaluation of the hypothalamic PRP-1 effect on mouse-isolated EAC cells on day 7 of tumor growth by H&E staining. Morphological changes of tumor cells (A) 24 and (B) 72 h after culture. (A) In control samples, numerous EAC cells linked with each other were detected at 24 h, whereas a decreased number of cells was observed with both doses of PRP-1. In the experimental samples, PRP-1-induced morphological changes were similar for both the two time-points of culture. Apoptotic membrane blebbing and apoptotic bodies (arrowheads), smaller and round-shaped cells with eosinophilic cytoplasm and condensed nuclei (pyknosis), and loss of reticular extensions and contacts with adjacent cells were observed. (B) Necrotic EAC cells containing no nuclei (karyolysis) or cells with lost membrane integrity (arrows) were mainly presented in the control samples after 72 h of culture, whereas few necrotic cells with lost plasma membrane integrity and released cell death products (arrows) were detected in the samples treated with PRP-1 for 72 h. Statistical data regarding the PRP-1 (0.1 and 1 µg/ml) effect on the apoptosis and necrosis in tumor cells treated for (C) 24 h and (D) 72 h were presented according to the H&E exclusion test in comparison with the findings in the untreated control cells. Data are presented as the mean \pm standard deviation (n=3), and represent ≥ 3 independent experiments. **P<0.01; ***P<0.001, significant difference compared to (C) the control at 24 h and (D) the control at 72 h. EAC, Ehrlich ascites carcinoma; PRP-1, proline-rich polypeptide 1; H&E, hematoxylin and eosin.

induced a statistically significant number of early apoptotic cells reaching 50.33% and late apoptotic cells (11.33%) on day 7 post-inoculation (Fig. 9B).

According to the literature data, a secondary form of necrosis has been demonstrated to occur in late apoptotic cells where apoptotic bodies undergo secondary necrotic changes and turn to detritus, taking mainly place *in vitro* when phagocytosis does not occur because of the absence of macrophages (38). Concomitantly, 53.34% inhibition of the viable number of cells caused by PRP-1 was observed.

On day 11 post-inoculation, incubation with 0.1 µg/ml PRP-1 caused a 58% increase in apoptotic cells and a 57.33% decrease in viable cells (Fig. 10B).

Immunohistochemical study. Using a PRP-1-antiserum, an immunohistochemical study was carried out to detect PRP-1

localization in the EAC cells and to examine PRP-1-triggered cell death (apoptosis/necrosis) on days 7 and 11 of tumor growth (Figs. 11 and 12). The results obtained detected no PRP-1-immunoreactivity (PRP-1-IR) in the control non-cultured EAC cells. No intracellular PRP-1-IR was detected in control EAC cells as well, after 24 h of culture, whereas the plasma membrane exhibited weak PRP-1-IR in the form of a narrow ring. In the experimental samples, the sub-membrane cytoplasm with dense PRP-1-IR was detected in the tumor cells exposed to 0.1 µg/ml PRP-1. However, on the 7 and 11th days of tumor growth, at 72 h after EAC cell culture, nuclear, as well as dense cytoplasmatic IR for PRP-1 was detected in tumor cells both in the untreated control and PRP-1-treated samples. Morphological changes of cells undergoing death-related processes (apoptosis and necrosis) were clearly observed, including release of PRP-1-IR intracellular

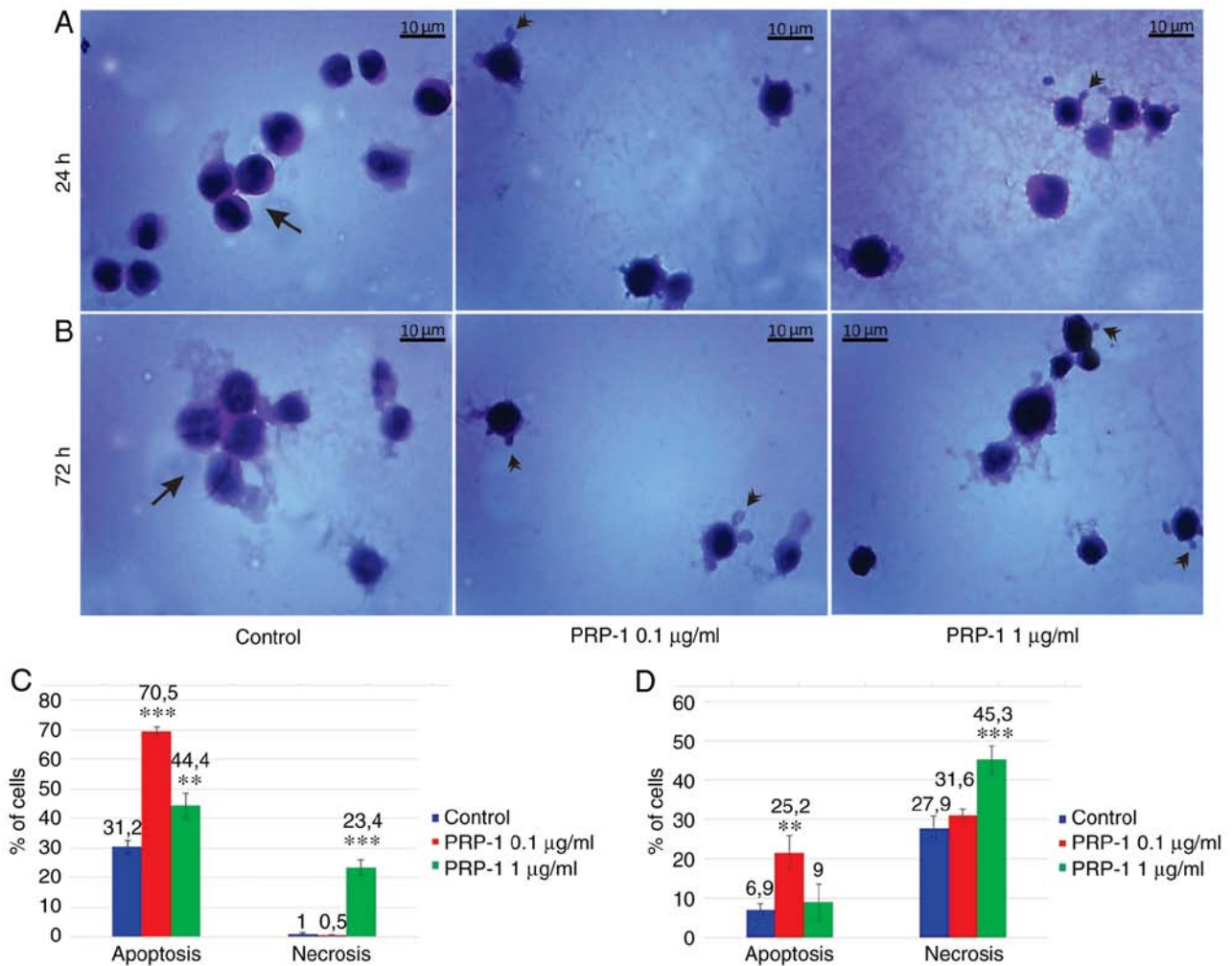


Figure 8. Histological evaluation of the hypothalamic PRP-1 effect on mouse-isolated EAC cells on the 11th day of tumor growth by H&E staining. Morphological changes of tumor cells at (A) 24 and (B) 72 h after culture. In the untreated control samples, tumor cells (arrows) with typical morphology were observed after both culture time-points. In comparison to cells in the control group, cells exposed to 0.1 and 1 µg/ml PRP-1 were smaller in size and exhibited a round shape. EAC cells with the apoptotic bodies (arrowheads) were observed having no contact to adjacent cells. Statistical data regarding the PRP-1 (0.1 and 1 µg/ml) effect on the apoptosis and necrosis in tumor cells treated for (C) 24 h and (D) 72 h was presented according to the H&E exclusion test in comparison with the findings in untreated control cells. Data are presented as the mean \pm standard deviation (n=3), and represent ≥ 3 independent experiments. **P<0.01; ***P<0.001, significant difference compared to (C) the control at 24 h and (D) the control at 72 h. EAC, Ehrlich ascites carcinoma; PRP-1, proline-rich polypeptide 1; H&E, hematoxylin and eosin.

contents from necrotic cells into the extracellular space, which was detected predominantly in the control samples, while PRP-1-immunoreactive (PRP-1-Ir) apoptotic cells with plasma blebs and apoptotic bodies were revealed mainly in the experimental samples.

Data of the statistical analysis on the PRP-1 cellular localization is presented in the Fig. 13. Thus, on the 7th day of inoculation, in the experimental samples exposed to 24 h 0.1 µg/ml PRP-1 (Fig. 13A) the sub-membrane cytoplasm with dense PRP-1-IR was detected in 46.5% of tumor cells in contrast to control cells. After 72 h of culture, nuclear localization of PRP-1 was detected in ~4% of the control cells and in 3.3% of 0.1 µg/ml PRP-1-treated tumor cells. The number of cells with cytoplasmic reactivity constituted 70.4 and 73.4% in the 1 and 0.1 µg/ml PRP-1 groups, respectively, in contrast to 32.6% in the control cells (Fig. 13B).

On the 11th day of inoculation in the untreated control samples at 24 h PRP-1-IR was mainly observed in the cytoplasmic perinuclear zone in ~10.1% of cells (Fig. 13C). At

72 h after EAC cell culture, strong cytoplasmic IR for PRP-1 was observed in tumor cells both in the control (48.1%) and PRP-1-treated (~40%) samples (Fig. 13D).

A nuclear counterstain method with DAPI fluorescent staining applied, confirmed the immunohistochemically detected PRP-1 nuclear localization in the cultured EAC cells both in the control and 0.1 µg/ml PRP-1-treated samples (Fig. 14).

Discussion

The cytostatic or antiproliferative effect of the hypothalamic PRP-1 in the human chondrosarcoma JJ012 cell line was previously demonstrated after PRP-1 treatment compared with chondrocyte culture, indicating that PRP-1 selectively targets malignant sarcoma cells and not benign cells (11). Unlike in chondrosarcoma, in glioblastoma, PRP-1 does not have any inhibitory activity on cell proliferation (12). The objective of the present morphological study was to

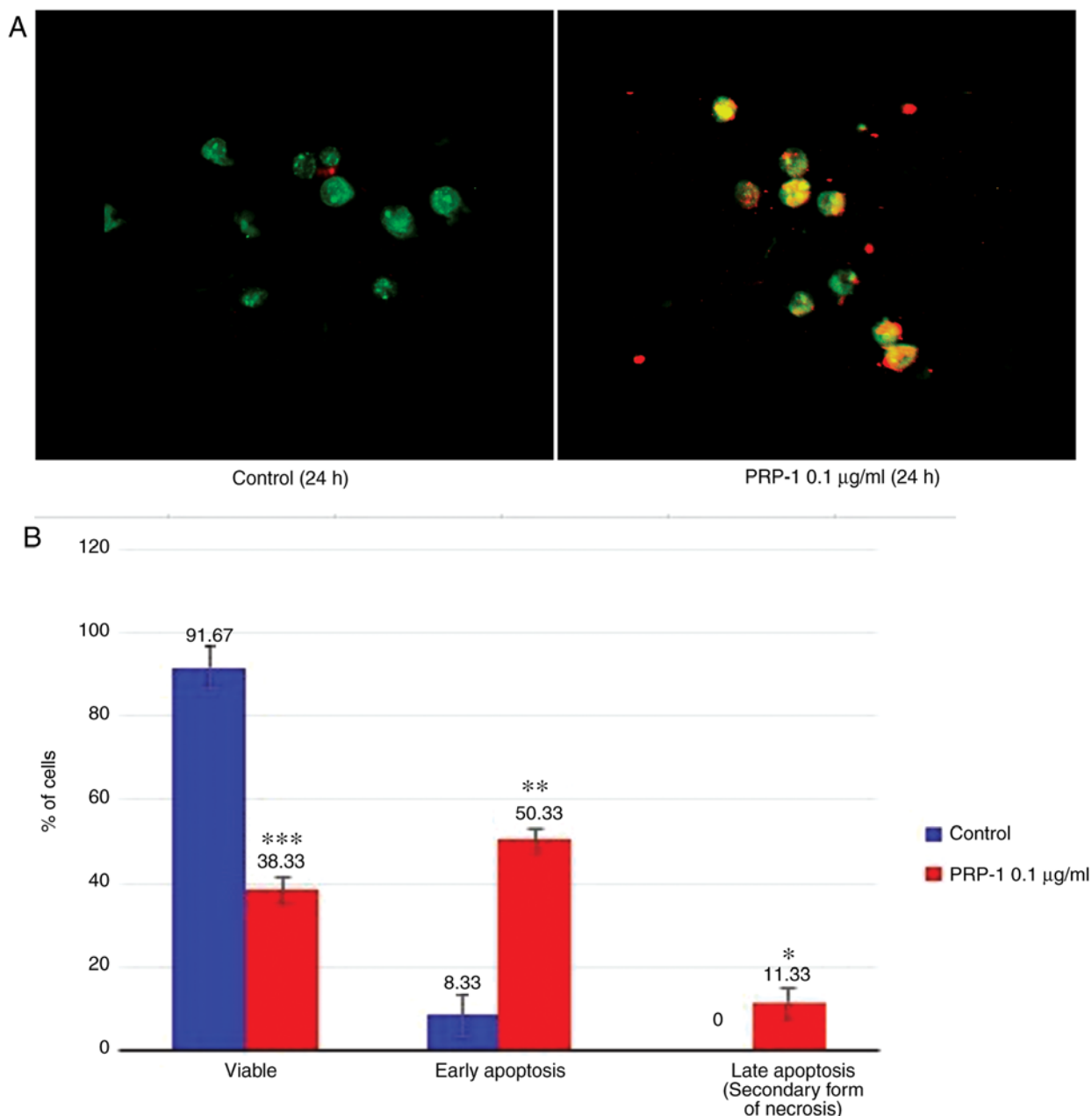


Figure 9. Analysis of apoptosis/necrosis in cultured mouse EAC cells exposed to the hypothalamic PRP-1 on the 7th day of tumor growth according to fluorescence detection with Annexin V-cyanine 3. (A) Viable EAC cultured cells (green) were detected 24 h after growing in the control untreated samples, although a number of necrotic nuclei (red) were also observed. In contrast to control samples, an increased number of early apoptotic cells (orange) was revealed 24 h after treatment with 0.1 µg/ml PRP-1. Fragments of necrotic nuclei (red) were clearly detected in late apoptotic cells. (B) The effect of PRP-1 on the apoptosis/necrosis of EAC cultured cells on the 7th day of tumor growth was evaluated by the Annexin V exclusion test. Statistical analysis of the data at 24 h clearly revealed a significant difference between the control (blue) and experimental samples (red). Treatment with 0.1 µg/ml PRP-1 led to a decreased number of viable cells and an increased number of early and late apoptotic cells. Data are presented as the mean ± standard deviation (n=3), and represent ≥3 independent experiments. *P<0.05; **P<0.01; ***P<0.001, significant difference compared to the control at 24 h. EAC, Ehrlich ascites carcinoma; PRP-1, proline-rich polypeptide 1.

investigate the antitumorigenic effect of PRP-1 against EAC cells to elucidate the underlying molecular mechanisms of action (cytostatic/antiproliferative or cytotoxic/apoptotic) on the aforementioned tumor cells.

In the present study data obtained by histological method with Tr-BI staining revealed an inhibitory effect of PRP-1 on the number of tumor cells and their viability observed 24 h after a single administration of PRP-1 in comparison with non-treated control samples. For example, on day 7 post-inoculation, the number of total cells was 5×10^6 , and increased to

8×10^6 , with viable cells comprising 88%, whereas in 0.1 µg/ml PRP-1-treated samples, the total number of cells decreased to 4×10^6 , 66% of which were viable cells. Thus, PRP-1 inhibited the growth of viable cells by 22%. On day 11 post-inoculation, the total number of cells increased from 5×10^6 to 6.5×10^6 , of which 93% were viable cells in the 24 h control. It is notable that there were no significant differences between the total number of EAC cells (5×10^6) exposed to 0.1 and 1 µg/ml PRP-1. As for the viable cells, in comparison with the percentage of inhibition observed in the control group, 0.1 µg/ml PRP-1 inhibited the

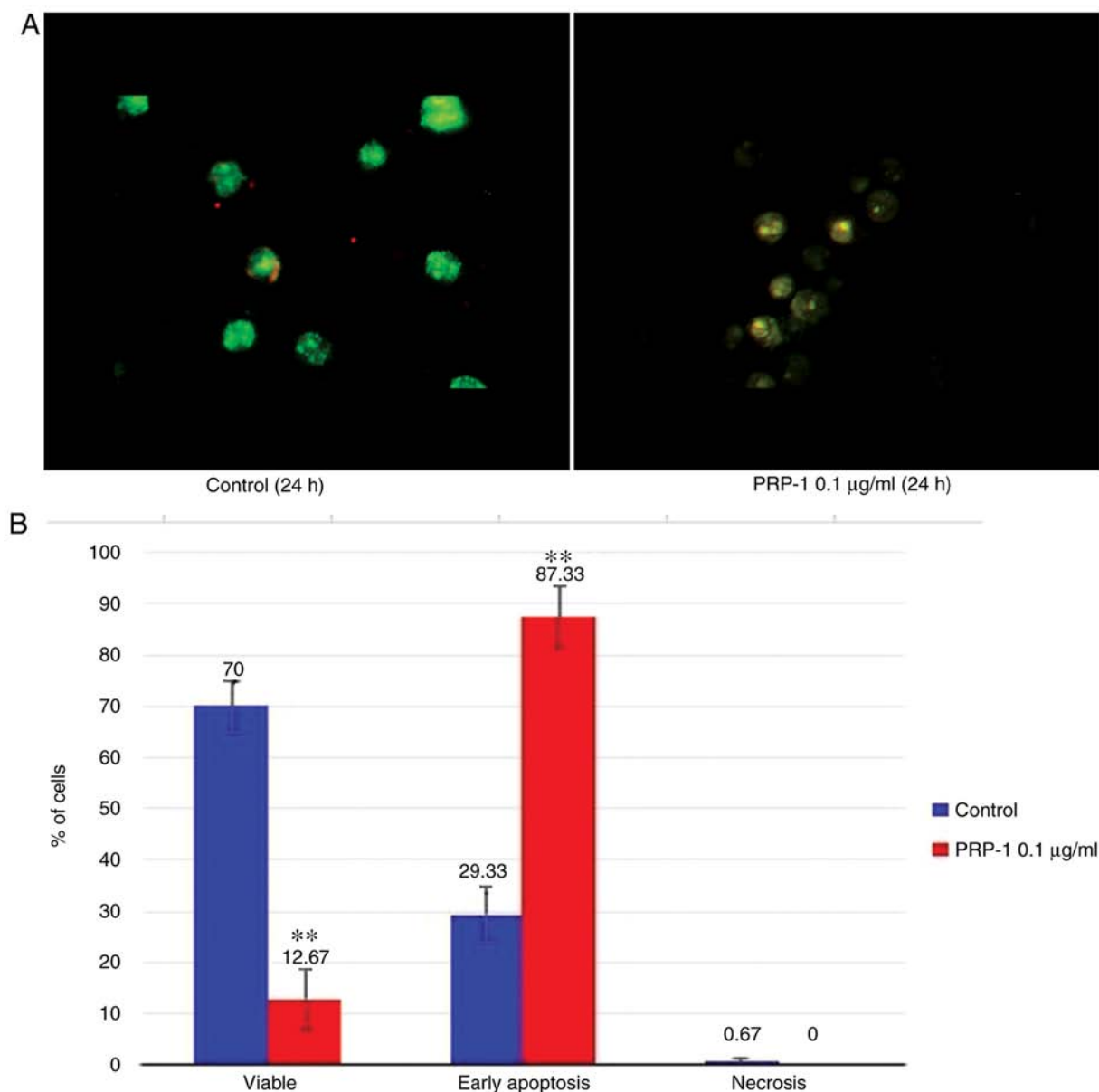


Figure 10. Analysis of apoptosis in cultured mouse EAC cells exposed to the hypothalamic PRP-1 on the 11th day of tumor growth by a fluorescence method involving Annexin V-cyanine 3 detection. (A) Viable EAC cells (green) were mainly observed in the 24 h control samples. After treatment with 0.1 µg/ml PRP-1, the plasma membrane and certain intracellular weakly-stained components could be indicative of early-stage apoptosis. (B) Effect of PRP-1 (red) on the apoptosis of cultured for 24 h EAC cells according to the Annexin V exclusion test. A significant increase in apoptotic cells was observed in comparison with that exhibited by the untreated control (blue). Data are presented as the mean \pm standard deviation (n=3), and represent ≥ 3 independent experiments. **P<0.01, significant difference compared to the control at 24 h. EAC, Ehrlich ascites carcinoma; PRP-1, proline-rich polypeptide 1.

viable cells by 49%. The results of different types of *in vitro* experiments carried out by our group, such as biochemical, immunological, morphological investigations confirmed that lower doses of PRP-1 were more effective than higher doses which was distinctive of several neuropeptides (10).

Histological methods with H&E, Papanicolaou and Giemsa staining were applied in order to examine the morphological features of the EAC control cells of mice on the 7 and 11th days of tumor growth. Staining with Papanicolaou revealed that EAC cells on the 11th day of tumor growth were markedly different from the tumor cells on the 7th day, as they were larger in size and exhibited pathological mitosis. Cells resembling macrophages were notably distinguished by strong staining with Giemsa.

Since histological methods with H&E staining are widely used in medical diagnosis and cancer detection, H&E staining was selected to study the morphological features of the control and PRP-1-exposed EAC cells, and to elucidate the underlying mechanisms of PRP-1 antitumor activity.

Based on the data regarding the cell shrinkage, membrane blebbing, chromosome condensation (pyknosis), nuclear fragmentation (karyorrhexis), as well as a predominant presence of apoptotic bodies (30-35), the apoptotic nature of PRP-1 was confirmed.

Conventional screening models for anticancer agents are geared toward the selection of cytotoxic drugs. It is highly desirable to have compounds that can cause cancer cell death via apoptosis, whereas the importance of cytostatic drugs,

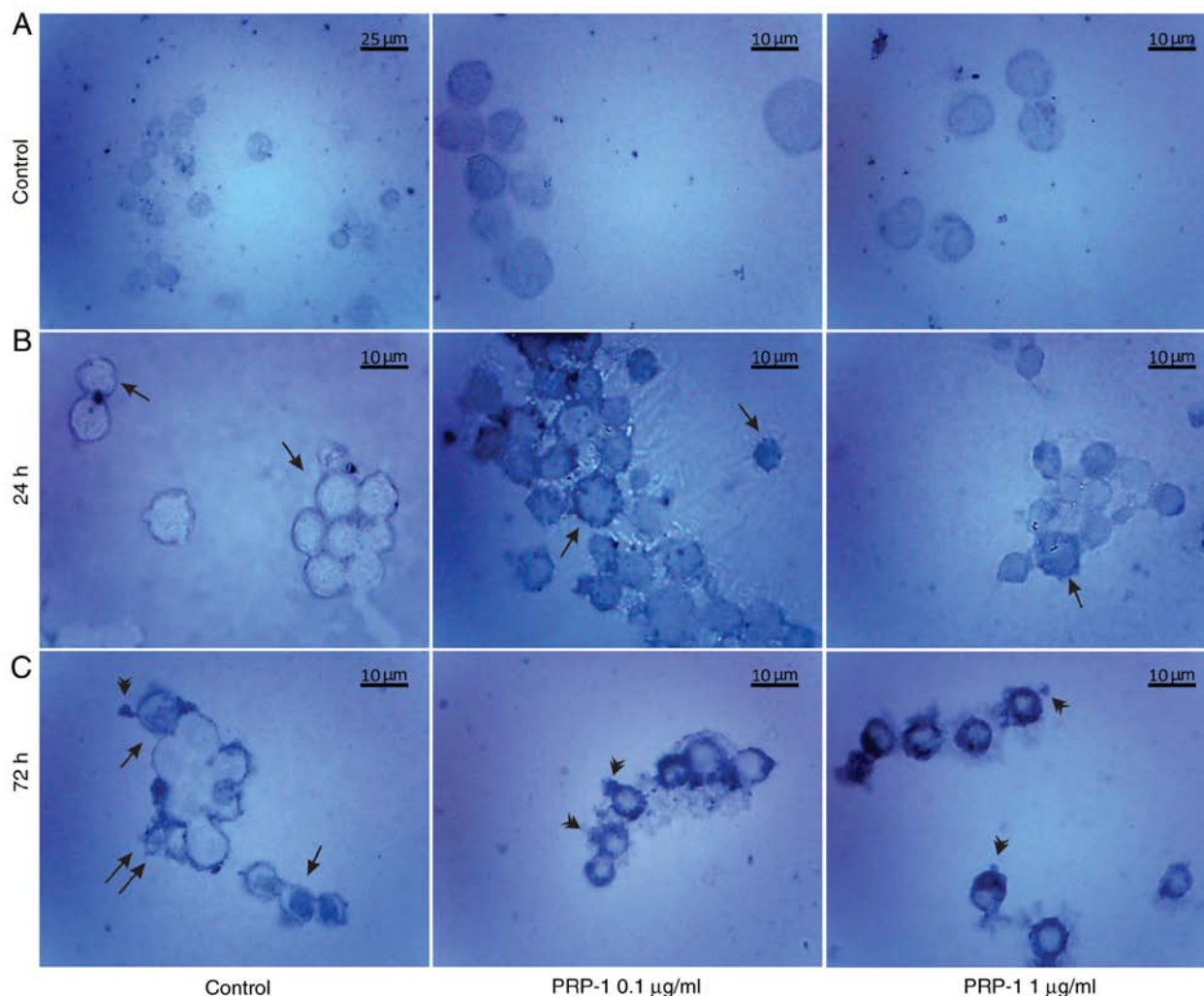


Figure 11. Immunohistochemical localization of the hypothalamic PRP-1 in cultured mouse EAC cells on the 7th day of tumor growth according to the ABC immunohistochemical method. (A) All microimages demonstrated no PRP-1-IR in EAC cells before culture (control). PRP-1-IR in tumor cells (B) at 24 h and (C) 72 h after culture. (B) No intracellular PRP-1-IR was detected in control EAC cells after 24 h of culture, whereas the plasma membrane exhibited weak PRP-1-IR in the form of a narrow ring (arrows). In experimental samples, the sub-membrane cytoplasm with dense PRP-1-IR was detected in the tumor cells (arrows) exposed to 0.1 $\mu\text{g/ml}$ PRP-1. (C) After 72 h of culture, nuclear localization of PRP-1 was detected in certain control (arrows) and PRP-1-treated (not shown) tumor cells. PRP-1-IR cytoplasm was released from necrotic control cells with lost membrane integrity (double arrows). The strong PRP-1-IR cytoplasm was revealed both in control (not demonstrated) and exposed to PRP-1 EAC cells. Notably, the apoptotic cells with the apoptotic bodies (arrowheads) also demonstrated strong PRP-1-IR cytoplasm. PRP-1, proline-rich polypeptide 1; EAC, Ehrlich ascites carcinoma; ABC, avidin-biotin complex; PRP-1-IR, PRP-1-immunoreactivity; PRP-1-Ir, PRP-1-immunoreactive.

particularly mTORC1 inhibitors, cannot be denied. In contrast to apoptosis, the membrane integrity is lost due to necrotic cellular death, accompanied by an uncontrolled release of products of cell death into the extracellular space (39-41). Data of the statistical analysis on the number of necrotic and apoptotic cells were included in the present study.

Typical morphological features of apoptotic cells can be observed using inverted phase contrast and fluorescence microscopy. In the present study, morphological data from the detection of apoptotic tumor cells indicated the apoptotic nature of PRP-1 in EAC cells. To verify this observation, a series of experiments were performed which focused on the determination of apoptosis in cultured tumor cells using an Annexin V-Cy3 apoptosis detection kit. Analysis of apoptosis by the Annexin V-Cy3 in the 7 day inoculated mice EAC-cultured cells exposed to 0.1 $\mu\text{g/ml}$ hypothalamic PRP-1 for 24 h revealed early apoptotic cells, as well as late

apoptotic cells, containing and surrounded by fragments of necrotic nuclei, in contrast to the numerous viable tumor cells detected in the untreated control samples. A secondary form of necrosis is known to occur in late apoptotic cells where apoptotic bodies undergo secondary necrotic changes and turn to detritus, taking mainly place *in vitro* when phagocytosis does not occur due to the absence of macrophages (38).

On day 11 of tumor growth after treatment with PRP-1, the cell plasma membrane and certain intracellular components manifested signs of early-stage apoptosis. Thus, the apoptotic effect of PRP-1 on EAC-cultured cells of the 7 day inoculated mice revealed a significant difference between the control and experimental samples, since PRP-1 induced a decrease in viable number of cells, and an increase the early and late apoptotic number of cells.

Apoptosis experiments indicated that 24 h of culture with PRP-1 induced a statistically significant increase in the

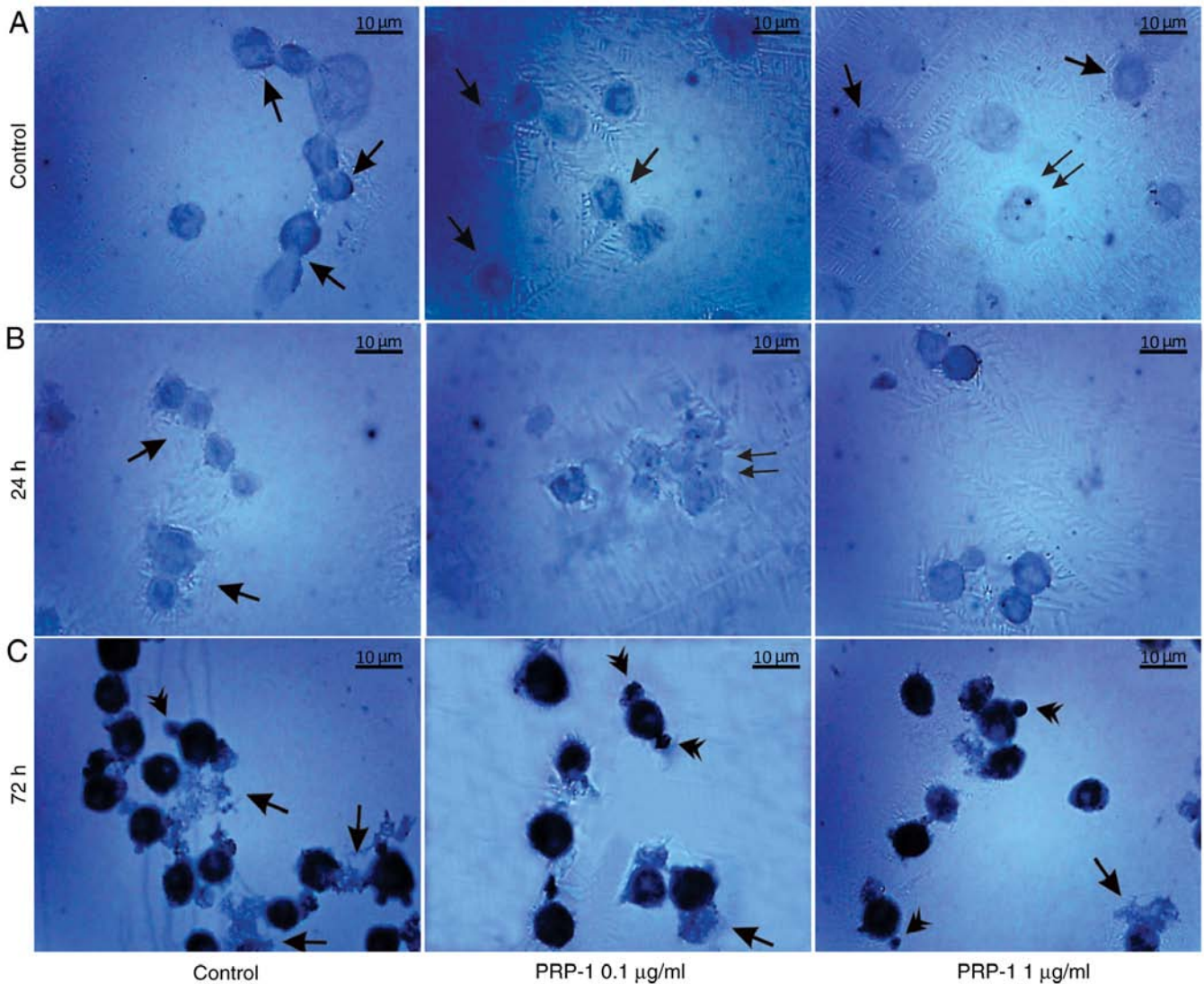


Figure 12. Immunohistochemical localization of the hypothalamic PRP-1 in cultured mouse EAC cells on the 11th day of tumor growth according to the ABC immunohistochemical method. (A) EAC control cells before culture, where PRP-1 was localized in the cell membrane, cytoplasm (arrows) and nucleoli (double arrows) of certain tumor cells. PRP-1-IR in the tumor cells (B) 24 h and (C) 72 h after their culture. (B) In the untreated control samples at 24 h, weak PRP-1-IR was mainly observed in the perinuclear zone of cell cytoplasm. In the experimental samples exposed to 0.1 $\mu\text{g/ml}$ PRP-1 for 24 h, PRP-1-IR was observed in the cells nucleoli (double arrows). (C) At 72 h after EAC cell culture, dense cytoplasmic IR for PRP-1 was detected in tumor cells both in the control and PRP-1-treated samples. Morphological changes of cells undergoing death-related processes (apoptosis and necrosis) were clearly observed, including release of PRP-1-IR intracellular contents from necrotic cells into the extracellular space, which was detected predominantly in the control samples (arrows), while PRP-1-IR plasma blebs and apoptotic bodies (arrowheads) were revealed mainly in the experimental samples. PRP-1, proline-rich polypeptide 1; EAC, Ehrlich ascites carcinoma; ABC, avidin-biotin complex; PRP-1-IR, PRP-1-immunoreactivity; PRP-1-Ir, PRP-1-immunoreactive.

number of early apoptotic cells, reaching 50.33% on day 7 post-inoculation, whereas day 11 post-inoculation, a 58.33% increase in the number of early apoptotic cells was detected. In conclusion, the PRP-1 effect was cellular-context dependent, and in EAC cells acted as a cytotoxic agent, causing programmed cell death type I apoptosis.

A series of experiments which aimed to elucidate the possible participation of PRP-1 in antitumorogenic processes were carried out by detecting the immunohistochemical localization of PRP-1 in the control and experimental EAC cells using an antibody against the synthetic hypothalamic polypeptide of interest.

On the 7th day of tumor growth, no PRP-1-IR was detected in the mice non-cultured control EAC cells. In the untreated control EAC cells cultured for 24 h, no intracellular PRP-1-IR

was detected, but the PRP-1-IR cell membrane (21%) was demonstrated in the form of a narrow ring. In the experimental samples exposed to 0.1 $\mu\text{g/ml}$ PRP-1, strong PRP-1-IR was observed in the cytoplasm (46.5%) and nucleoli (10%) of the total number of tumor cells.

In the control cells, as well as in the PRP-1-treated samples after 72 h of incubation, nuclear localization of PRP-1 was detected in 3.3-4% of tumor cells, which was statistically not significant. However, the number of cells exposed to PRP-1 with cytoplasmic PRP-1-IR constituted 73.4%, in contrast to 32.6% of the control cells. Notably, dense PRP-1-IR was noticed in 25% of apoptotic cells with the membrane blebbing, in contrast to 4% of the untreated control cells.

Immunohistochemically-detected PRP-1 nuclear localization in the cultured EAC cells both in the control and

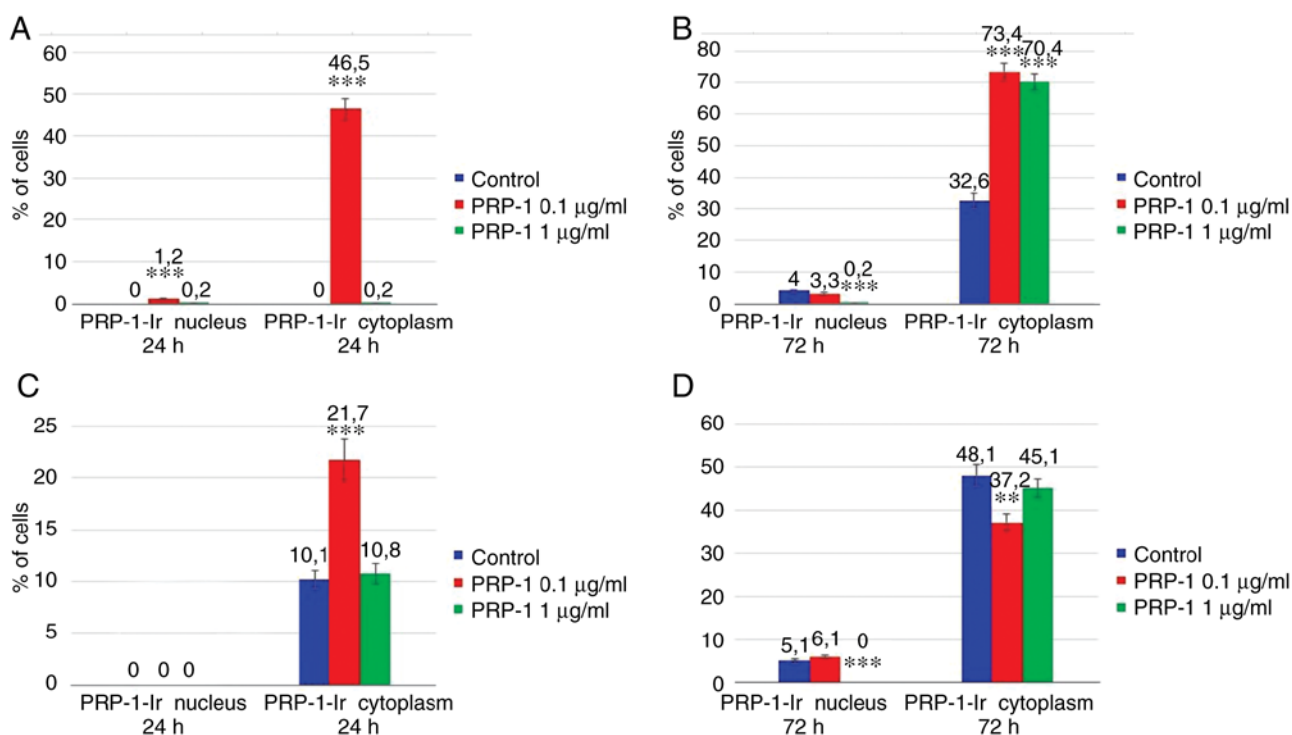


Figure 13. Statistical data regarding the PRP-1 localization in the cultured (A and C) 24 h and (B and D) 72 h control, 0.1 and 1 µg/ml PRP-1-treated cells of days 7 and 11 of tumor growth in mice are presented according to the immunohistochemical exclusion test. Data are presented as the mean ± standard deviation (n=3), and represent ≥3 independent experiments. **P<0.01 and ***P<0.001, significant difference compared to (A and C) the control at 24 h and (B and D) the control at 72 h. PRP-1, proline-rich polypeptide 1; PRP-1-Ir, PRP-1-immunoreactive.

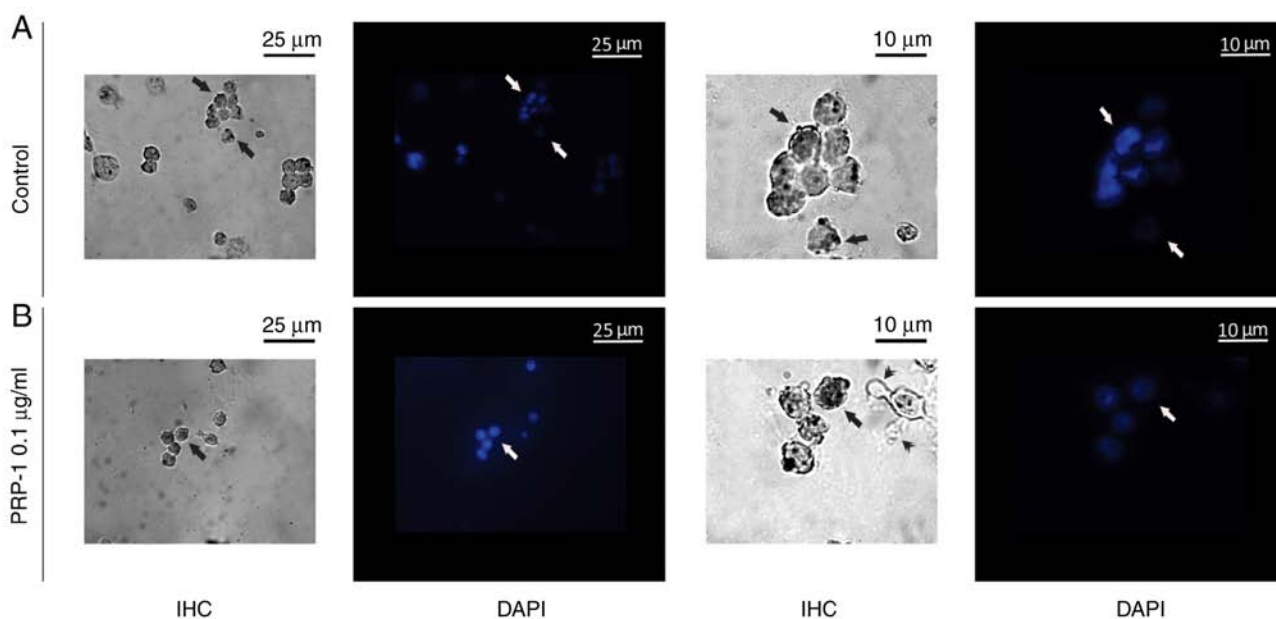


Figure 14. Detection of the nuclei in the mouse EAC-cultured cells according to the ABC immunohistochemical method and nuclear counterstain method with DAPI fluorescent dye. Seventy-two hours after EAC cell culture, PRP-1-Ir nuclei (arrows) were detected in the (A) control and (B) 0.1 µg/ml PRP-1-treated tumor cells; an apoptotic tumor cell with the isolated apoptotic bodies is well demonstrated (arrowheads). DAPI counterstained nuclei (arrows) in the (A) control and (B) 0.1 µg/ml PRP-1-treated tumor cells were revealed. EAC, Ehrlich ascites carcinoma; ABC, avidin-biotin complex; PRP-1-Ir, PRP-1-immunoreactive; PRP-1, proline-rich polypeptide 1; DAPI, 4',6-diamidino-2-phenylindole.

PRP-1-treated samples was confirmed by the nuclear counterstain method with DAPI fluorescent staining. In mice inoculated for 11 days, PRP-1-IR was different in control-EAC cells before their culture compared with that of cells after 7 days of

tumor growth. In certain EAC cells, weak positivity for PRP-1 was observed in the cell membrane (15%) and the perinuclear zone of the cytoplasm (9%). In the experimental samples exposed to 0.1 µg/ml PRP-1 for 24 h, PRP-1-IR was observed

in the nucleoli of the cultured tumor cells. Morphological changes of cells undergoing death-related processes (apoptosis and necrosis) were clearly observed 72 h after EAC cell culture, as manifested by markedly dense cytoplasmatic IR for PRP-1 both in the control (48%) and PRP-1-treated (~40%) samples. PRP-1-IR cell membrane blebs and apoptotic bodies were observed in close contact to EAC cells mainly in the experimental samples, indicating that apoptosis was involved in the underlying mechanisms of PRP-1 antitumorigenic action. PRP-1-IR was detected in the nucleus and cytoplasm of EAC cells cultured for 72 h in both control (untreated) and experimental (PRP-1-treated) samples, which may be explained by the possible biosynthesis of endogenous PRP-1 in the studied cancer cells. This hypothesis is in agreement with previous immunohistochemical data on the detection of PRP-1 in the nuclei of neural cells of labyrinthectomized rats (42), motoneurons of spinal cord hemisectioned rats in response to cobra venom administration (43) and bone marrow-derived immune system cells of immobilized rats (44).

The time-dependent quantity of PRP-1 expression in the blood samples of PRP-1-injected rats was demonstrated previously (45). Thus, PRP-1 has been quantified in intact (normal) rat blood serum samples, which was estimated to be ~1.78 ng/ml, with a significant increase in PRP-1 concentration (36.76 ng/ml) in blood samples at 5 h post-PRP-1 i/p injection. However, the peptide concentration in the blood decreased at day 2 post-injection to 3.111 ng/ml, similar to that found in the control, which was explained by proteolytic breakdown of the peptide. This assumption has been based on the recently revealed data indicating PRP-1 as a new natural substrate for DPPs (46) that are widely expressed on the surface of the lymphocytes in the blood plasma, substrates of which are chemokines, hormones, neuropeptides, and growth factors (47,48).

In summary, the present immunohistochemical results revealed PRP-1 localization in the nucleus and cytoplasm of both untreated control and PRP-1-exposed experimental EAC cells cultured for 72 h, which can be indicative of endogenous PRP-1 synthesis. Notably, our group previously reported the detection of PRP-1 receptors in the nuclei of cancer cells (15). Further *in vitro* and *in vivo* experiments are required to identify the involvement of particular caspases in apoptosis and to elucidate other PRP-1-triggered molecular pathways leading to cancer cell death.

Acknowledgements

Authors would like to thank the Miami Center of Orthopaedic Research and Education (Miami, FL, USA). Ehrlich Ascites Carcinoma (EAC) cells were kindly provided by Senior Researcher Hrachya Stepanyan from the laboratory of Toxicology and Experimental Chemotherapy, Institute of Fine Organic Chemistry, NAS, Armenia.

Funding

The present study was supported in part by a gift from Ratcliffe Foundation to the Miami Center of Orthopaedic Research and Education and the Buniatian Institute of Biochemistry NAS of the Republic of Armenia.

Availability of data and materials

All data generated or analyzed during this study are included in this published article.

Authors' contributions

SA, IS, NT, NK, TD and KG were involved in the study design and contributed to the preparation of the manuscript and data analysis. AS and RA were in charge of the fluorescence microscopy, statistical and experimental data analysis at Yerevan State University. GC and SC contributed to the peptide synthesis. All authors read and approved the final manuscript and agree to be accountable for all aspects of the research in ensuring that the accuracy or integrity of any part of the work are appropriately investigated and resolved.

Ethics approval and consent to participate

The Institutional Animal Ethics Committee of the Institute of Biochemistry after H.Buniatian, NAS, RA (IRB 0001621; IORG0009782) provided approval for the use of the animals in the present study.

Patient consent for publication

Not applicable

Competing interests

The authors declare that they have no competing interests.

References

- Galoyan A: Neurochemistry of brain neuroendocrine immune system: Signal molecules. *Neurochem Res* 25: 9-10, 2000.
- Markossian KA, Gurvitz BY and Galoyan AA: Isolation and chemical identification of new peptides from neurosecretory granules of hypothalamus. *Neurokhimiya* 16: 22-25, 1999.
- Davtyan TK, Manukyan HA, Mkrtchyan NR, Avetisyan SA and Galoyan AA: Hypothalamic proline-rich polypeptide is a regulator of oxidative burst in human neutrophils and monocyte. *Neuroimmunomodulation* 12: 270-284, 2005.
- Galoyan AA, Sarkissian JS, Sulkhanyan RM, Chavushyan VA, Avetisyan ZA, Avakyan ZE, Gevorgyan AJ, Abrahamyan DO and Grigorian YKh: PRP-1 protective effect against central and peripheral neurodegeneration following n. ischiadicus transection. *Neurochem Res* 30: 487-505, 2005.
- Galoian K, Luo S, Qureshi A, Patel P, Price R, Morse A, Chailyan G, Abrahamyan S and Temple HT: Proline rich polypeptide-1 and inflammatory pathway signaling in chondrosarcoma. *Mol Clin Oncol* 5: 618-624, 2016.
- Durgaryan AA, Matevosyan MB, Seferyan TY, Sargsyan MA, Grigoryan SL, Galoian KA and Galoyan AA: The protective and immunomodulatory effects of hypothalamic proline-rich polypeptide galarmin against methicillin-resistant *Staphylococcus aureus* infection in mice. *Eur J Clin Microbiol Infect Dis* 3: 2153-2165, 2012.
- Galoyan AA, Korochkin LI, Rybalkina EJ, Pavlova GV, Saburina IN, Zaraiski EI, Galoyan NA, Davtyan TK, Bezirganyan KB and Revishchin AV: Hypothalamic proline-rich polypeptide enhances bone marrow colony-forming cell proliferation and stromal progenitor cell differentiation. *Cell Transplant* 17: 1061-1066, 2008.
- Galoyan KA, Scully SP and Galoyan AA: Myc-Oncogene inactivating effect by proline rich polypeptide (PRP-1) in chondrosarcoma. *Neurochem Res* 34: 379-385, 2009.

9. Galoian K, Temple TH and Galoyan A: Cytostatic effect of the hypothalamic cytokine PRP-1 is mediated by its inhibition of mTOR and cMyc in high grade metastatic chondrosarcoma. *Neurochem Res* 36: 812-818, 2011.
10. Galoian KA, Temple HT and Galoyan AA: Cytostatic effect of novel mTOR inhibitor, PRP-1 in MDA231 (ER-) breast carcinoma cell line. The cytokine inhibits mesenchymal tumors. *Tumor Biol* 32: 745-751, 2011.
11. Galoian KA, Guettouche T, Issac B, Qureshi A and Temple HT: Regulation of onco and tumor suppressor miRNAs by mTORC1 inhibitor PRP-1 in human chondrosarcoma. *Tumour Biol* 35: 2335-2341, 2014.
12. Galoian K, Qureshi A, Dippolito G, Schiller PC, Molinari M, Johnstone AL, Brothers SP, Paz AC and Temple HT: Epigenetic regulation of embryonic stem cell marker miR302C in human chondrosarcoma as determinant of antiproliferative activity of proline rich polypeptide-1. *Lnt J Oncol* 47: 465-472, 2015.
13. Galoian K, Qureshi A, Wideroff G and Temple HT: Restoration of desmosomal junction protein expression and inhibition of H3K9-specific histone demethylase activity by cytostatic proline-rich polypeptide-1 leads to suppression of tumorigenic potential in human chondrosarcoma cells. *Mol Clin Oncol* 3: 171-178, 2015.
14. Chailakhyan RK, Gerasimov YV, Chailakhyan MR and Galoyan AA: Proline-rich hypothalamic polypeptide has opposite effects on the proliferation of human normal bone marrow stromal cells and human giant-cell tumour stromal cells. *Neurochem Res* 35: 934-939, 2010.
15. Galoian K, Abrahamyan S, Chailyan G, Qureshi A, Patel P, Metsler G, Moran A, Sahakyan I, Tumasyan N, Lee A, *et al*: Toll like receptors TLR1/2, TLR6 and MUC5B as binding interaction partners with cytostatic proline rich polypeptide 1 in human chondrosarcoma. *Int J Oncol* 52: 139-154, 2018.
16. Galoian K, Scully S, McNamara G, Flynn P and Galoyan A: Antitumorigenic effect of brain proline rich polypeptide-1 in human chondrosarcoma. *Neurochem Res* 34: 2117-2121, 2009.
17. Jaganathan SK, Mondhe D, Wani ZA, Pal HC and Mandal M: Effect of honey and eugenol on Ehrlich ascites and solid carcinoma. *J Biomed Biotechnol*: 989163, 2010.
18. Frajacom FT, de Souza Padilha C, Marinello PC, Guarnier FA, Cecchini R, Duarte JA and Deminice R: Solid Ehrlich carcinoma reproduces functional and biological characteristics of cancer cachexia. *Life Sci* 162: 47-53, 2016.
19. Mondal A, Singha T, Maity TK and Pal D: Evaluation of anti-tumor and antioxidant activity of melothriaheterophylla (Lour.). *Cogn. Indian J Pharm Sci* 75: 515-522, 2013.
20. Strober W: Trypan blue exclusion test of cell viability. *Curr Protoc Immunol* 111: A3B1-A3B3, 2015.
21. Fischer A, Jacobson KA, Rose J and Zeller R: Hematoxylin and eosin staining of tissue and cell sections. *CSH Protoc* pdb. prot4986, 2008.
22. Redginal H: Giemsa preparation for staining blood films. *Science* 86: 548, 1937.
23. Deshpande AK, Bayya P and Veeragandham S: Comparative study of Papanicolaou stain (PAP) with rapid economic acetic acid papanicolaou stain (REAP) in cervical cytology. *J Evolution of Med Dental Sci* 4: 7089-7095, 2015.
24. Farinacci M: Improved apoptosis detection in ovine neutrophils by annexin V and carboxyfluorescein diacetate staining. *Cytotechnology* 54: 149-155, 2007.
25. Szkaradek N, Sypniewski D, Waszkielewicz AM, Gunia-Krzyżak A, Galilejczyk A, Gałka S, Marona H and Bednarek I: Synthesis and in vitro evaluation of the anticancer potential of new aminoalkanol derivatives of xanthone. *Anticancer Agents Med Chem* 16: 1587-1604, 2016.
26. Hsu SM, Roine L and Farger H: Use of avidin-biotin-peroxidase (ABC) in immunoperoxidase techniques: comparison between ABC and unlabelled antibody (PAP) procedures. *J Histochem Cytochem* 29: 577-580, 1981.
27. Ambrosius X: Obtaining of antisera from different animals. In: *Immunological methods*. Frimel HG (ed). pp14-15, 1987.
28. Bret-Dibat JL, Zouaoui D, Déry O, Zerari F, Grassi J, Maillet S, Conrath M and Couraud JY: Antipeptide polyclonal antibodies that recognize a substance P-binding site in mammalian tissues: A biochemical and immunocytochemical study. *J Neurochem* 63: 333-343, 1994.
29. Engvall E: Enzyme immunoassay ELISA and EMIT. *Methods Enzymol* 70: 419-439, 1980.
30. Kasper DL and Zaleznik DF: Gas gangrene, antibiotic associated colitis, and other Clostridial infections. In Stone RM. *Harrison's principles of internal medicine self-assessment and board review*. Med Pub Div 922-927, 2001.
31. Andrade R, Crisol L, Prado R, Boyano MD, Arluzea J and Arechaga J: Plasma membrane and nuclear envelope integrity during the blebbing stage of apoptosis: A time-lapse study. *Biol Cell* 102: 25-35, 2009.
32. Shimizu T, Maeno E and Okada Y: Prerequisite role of persistent cell shrinkage in apoptosis of human epithelial cells. *Sheng Li Xue Bao* 59: 512-516, 2007.
33. Somasekharan SP, Koc M, Morizot A, Micheau O, Sorensen PH, Gaide O, Andera L and Martinou JC: TRAIL promotes membrane blebbing, detachment and migration of cells displaying a dysfunctional intrinsic pathway of apoptosis. *Apoptosis* 18: 324-336, 2013.
34. Nagata S: Apoptotic DNA fragmentation. *Exp Cell Res* 256: 12-18, 2000.
35. Nagata S, Nagase H, Kawane K, Mukae N and Fukuyama H: Degradation of chromosomal DNA during apoptosis. *Cell Death Differ* 10: 108-116, 2003.
36. Fadok VA, Bratton DL and Henson PM: Phagocyte receptors for apoptotic cells: Recognition, uptake and consequences. *J Clin Invest* 108: 957-962, 2001.
37. Henson PM, Bratton DL and Fadok VA: Apoptotic cell removal. *Curr Biol* 11: R795-R805, 2001.
38. Shacter E, Williams JA, Hinson RM, Senturker S and Lee YJ: Oxidative stress interferes with cancer chemotherapy: Inhibition of lymphoma cell apoptosis and phagocytosis. *Blood* 96: 307-313, 2000.
39. Niles AL, Moravec RA and Riss TL: In vitro viability and cytotoxicity testing and same-well multi-parametric combinations for high throughput screening. *Curr Chem Genomics* 3: 33-41, 2009.
40. Proskuryakov SY, Konoplyannikov AG and Gabai VL: Necrosis: A specific form of programmed cell death? *Exp Cell Res* 283: 1-16, 2003.
41. Kroemer G, Galluzzi L, Vandenabeele P, Abrams J, Alnemri ES, Baehrecke EH, Blagosklonny MV, El-Deiry WS, Golstein P, Green DR, *et al*: Classification of cell death: Recommendations of the nomenclature committee on cell death. *Cell Death Differ* 16: 3-11, 2009.
42. Tumasyan N, Sahakyan I, Kocharyan N, Galoyan K and Abrahamyan S: Effect of the physiologically active compounds on rat brain plasticity under the stress. *Materials of the XIV International scientific ecological. Conference*: 240-242, 2016.
43. Abrahamyan SS, Meliksetyan IB, Chavushyan VA, Aloyan ML and Sarkissian JS: Protective action of snake venom *Naja Naja Oxiana* at spinal cord hemisection. *Ideggyogy Sz* 60: 148-153, 2007.
44. Abrahamyan SS, Sahakyan IK, Meliksetyan IB, Tumasyan NV, Badalyan BY and Galoyan AA: Histochemical and immunohistochemical study of morphofunctional state of brain and bone marrow cell structures of rats under stress. *N Armenian Med J* 5: 60-68, 2011.
45. Abrahamyan SS, Davtyan TK, Khachatryan AR, Tumasyan NV, Sahakyan IK, Harutyunyan HA, Chailyan SG and Galoyan AA: Quantification of the hypothalamic proline rich polypeptide-1 in rat blood serum. *Neirokimiya* 31: 47-53, 2014.
46. Antonyan AA, Sharoyan SG, Mardanyan SS and Galoyan AA: Proline-rich cytokine from neurosecretory granules: A new natural substrate for dipeptidyl peptidase IV. *Neurochem Res* 36: 34-38, 2011.
47. Mentlein R: Proline residues in the maturation and degradation of peptide hormones and neuropeptides. *FEBS Lett* 234: 251-256, 1988.
48. Yaron A and Naider F: Proline-dependent structural and biological properties of peptides and proteins. *Crit Rev Biochem Mol Biol* 28: 31-81, 1993.



This work is licensed under a Creative Commons Attribution-NonCommercial-NoDerivatives 4.0 International (CC BY-NC-ND 4.0) License.